DNV·GL

PTIL - KONSTRUKSJONSSIKKERHET I ARKTISKE OMRÅDER (ST5)

Glacial Ice Impact

Petroleumstilsynet

Report No.: 2017-0425, Rev. 2
Document No.: 1115LU5A-19
Date: 2018-03-08
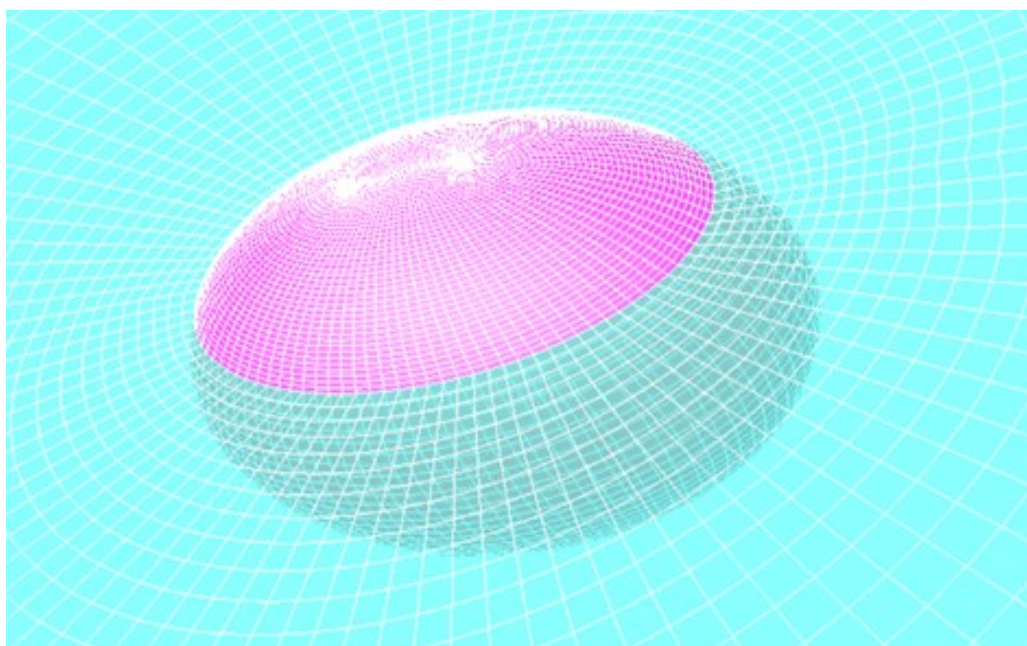
Project name:	Ptil - Konstruksjonssikkerhet i arktiske områder (ST5)	DNV GL AS Oil & Gas Environmental Loading &
Report title:	Glacial Ice Impact	Response
Customer:	Petroleumstilsynet, Postboks 599	P.O. Box 300
	4003 STAVANGER	1322 Høvik
	Norway	Norway
Customer contact:	Marita Halsne	Tel: +47 67 57 99 00
Date of issue:	2018-03-08	
Project No.:	10043532	
Organisation unit:	Environmental Loading & Response	
Report No.:	2017-0425, Rev. 2	
Document No.:	1115LU5A-19	

Applicable contract(s) governing the provision of this Report: Kontrakt 06566

Objective: The main objective of this study was to clarify the relevance of the inherent capacity of a facility to withstand a ship impact when considering an impact with glacial ice.

Prepared by:	Verified by:	Approved by:
Ole-Christian Ekeberg Senior Engineer	Arne Nestegård Chief Specialist	Florus Korbijn Head of Section
Olga Shipilova Senior Engineer		
Jørn Birknes-Berg Principal Specialist		
Rolf Lande Principal Engineer		
Alte Johansen Senior Principal Engineer		

DNV GL Distribution:	Keywords:
☒ Unrestricted distribution (internal and external)	Arctic, structural safetety, semi-submersible, PSA, glacial ice, rules, stability, icebergs, standards
☐ Unrestricted distribution within DNV GL Group	
☐ Unrestricted distribution within DNV GL contracting party	
☐ No distribution (confidential)	

Rev. No.	Date	Reason for Issue	Prepared by	Verified by	Approved by
0	2017-09-29	First issue	OCEK, OSHI, RHEL, ATLEJ, JBIR	ANE	KORB
1	2018-01-12	Second issue	OCEK, RHEL, ATLEJ, JBIR, YZANG	ANE	KORB
2	2018-03-08	Third issue	OCEK, JBIR	ANE	KORB

Table of contents

1 EXECUTIVE SUMMARY

DNV GL was given the task by the Petroleum Safety Authority to give an overview of knowledge and knowledge gaps related to structural safety in arctic areas. The northernmost blocks in the 23rd licensing round are at 74°N and the physical environment in this area differs, in parts of the year, from other areas on the Norwegian Continental Shelf where there is oil and gas activity today.

The first phase of this project discussed cold climate challenges, including technical challenges and weaknesses in rules and standards, and how these challenges are relevant to structural safety of drilling or production units operating in the Barents Sea area. The results from phase 1 are documented in the report 'Aspect of structural safety in the Barents Sea' [1].

One of the main findings from phase 1 was that all facilities operating on the Norwegian Continental Shelf are designed for ship collisions based on requirements in regulations. This means that they have some inherent capacity to withstand impacts with sea ice and glacial ice. However, during impact with sea ice and glacial ice, the impact energies and the exposed parts of the structure might be different from those relevant to ship impacts.

The main objective of this study was to assess whether impacts between smaller pieces of glacial ice and a floating facility can be acceptable because of the facility's capacity to withstand a ship impact. In the assessment, pieces of glacial ice with waterline less than 15 m have been applied. These are categorized either as growlers or bergy bits. For an ice management system, the possibility of successfully detecting glacial ice in waves increases with its waterline length. Measures to avoid interaction with glacial ice can be taken only by detecting the glacial ice in due time.

As an example, interaction between a semi-submersible and glacial ice was investigated. It should be noted that this study does not consider the probability of the combination of an interaction with glacial ice and the sea state. The interaction of glacial ice with the facility is analyzed for three specified sea states with annual probability of exceedance of 10^{-2}. In addition, analysis is done for one glacial ice shape in sea states with annual probability 10^{-1} and 0.63. Without loss of generality the shape of the glacial ice was simplified to be either spheroid or cuboid.

To estimate the impact energy and area of impact, wave radiation/diffraction program Wadam, was used. Wadam is a software tool for analyzing fixed and floating objects in waves. The Wadam analysis shows that the vertical extent assumed for ship impact is not sufficient to cover the possible extent of damage resulting from interaction between glacial ice and a semi-submersible. Even though a 100-year sea state was used as basis the results regarding vertical extent are conclusive. Further work is required to propose limits for the vertical extent of damage to be considered but the results show that the impact may occur both above and below the limits used for ship impact assessments.

For ship impact, it is assumed that impact only occur on the outer perimeter of the facility. This may not be sufficient for impacts with glacial ice. Glacial ice comes in many sizes and shapes and may protrude in-between the legs of a semi-submersible. In such a case, it may interact with structural elements not required to withstand ship impacts. The possibility for damage on more than two compartments has not been assessed in this study but the variability of the shapes and sizes of glacial ice suggests that a damage in more than two compartments cannot be excluded.

For ship impact the horizontal penetration of damage shall be assumed to be 1.5 m, this may not be sufficient for glacial ice impact. A finite element analysis which assumes that all dissipation of energy goes into the facility, shows that relatively low impact energies may cause significant penetration. The estimated horizontal penetration depth depends on the geometry of the glacial ice, the energy available for deformation and the pressure exerted by the ice on the facility.

The main options to evaluate a facility's ability to resist ice collision is to simulate the Glacial ice as

- Rigid objects

- Pressure as function of time

The resistance results must then be compared with predicted ice pressure, e.g. pressure-area model results as shown herein.

Both methods are simplifications and assumes that the structure response and the ice response to the collision can be threated independently. When a "strength design" is aimed for, simulation the ice load using pressure as function of time is a good approximation. There is considerable uncertainty associated with the pressure-area relation for glacial ice and further work is required to conclude on this matter.

Integrated analyses, where FE models, Smoothed-Particle Hydrodynamics (SPH) or similar are utilized to describe also the crushing of the ice have been attempted. Data needed to calibrate such advanced models are however scarce, and the models are thus not evaluated to be suited for design against ice collision so far.

The present study has assumed linear radiation and diffraction theory for solving the global response of the ship and glacial ice. However, the selected glacial ice shapes may be completely submerged for high waves and certain wave periods. Then, the water plane area and the vertical restoring coefficient stiffness (C_{33}) vanish, resulting in a non-linear motion. This is not captured by the applied linear analysis tool. To address non-linear hydrodynamic effects, a time domain simulation with the program Wasim is carried out. The large spheroid is chosen since the water plane area changes significantly during one wave cycle for this geometry. Compared with the Wadam analysis, the non-linear analysis gives an increase in heave motion and horizontal velocity. Also, it is observed that the spheroid may be completely submerged and the time series for pitch motion show that the spheroid may tip over and rotate 360 degrees.

The main findings in this study are the following:

- vertical extent of damage for semi-submersibles, assumed for ship impact assessment, is not sufficient for glacial ice impact assessments

- structural components assumed not to be exposed to ship impact may still be exposed to impact from glacial ice

- the horizontal penetration of damage may exceed 1.5 m which is the minimum requirement for ship impact

- the pressure-area formulation used to assess glacial ice impact is associated with uncertainty that should be considered in estimating glacial ice loads

2 INTRODUCTION

2.1 Background and objectives

DNV GL was given the task by the Petroleum Safety Authority to give an overview of knowledge and knowledge gaps related to structural safety in arctic areas. The northernmost blocks in the 23rd licensing round are at 74°N and the physical environment in this area differs, in parts of the year, from other areas on the Norwegian Continental Shelf where there is oil and gas activity today.

The first phase of this project discusses cold climate challenges, including technical challenges and weaknesses in rules and standards, and how these challenges are relevant to structural safety of drilling or production units operating in the Barents Sea area. The result from phase 1 are documented in the report 'Aspect of structural safety in the Barents Sea' [1].

One of the main findings from phase 1 was that all facilities operating on the Norwegian Continental Shelf are designed for ship collisions because of requirements in existing rules and standards. This means that they have some inherent capacity to withstand impacts with sea ice and glacial ice. However, during impact with sea ice and glacial ice, the impact energies and the exposed parts of the structure might be different from those relevant to ship impacts.

The study also identified a need for further work required to: (i) understand ice-structure interaction during broken ice conditions, (ii) understand the mechanics of glacial ice impacts, and (iii) quantify the uncertainty involved in such interactions. In particular, the study suggests, that such knowledge should be used to perform a number of structural reliability assessments, perhaps leading to a region-specific calibration of the partial action factor associated with ice design loads applicable to facilities in the Barents Sea.

This report is the result of one of two tasks in the second phase of the project (referred to by the PSA as the 'hovedstudie/kunnskapsinnhenting'). This report studies the relevance of the inherent capacity to withstand a ship impact when considering an impact with glacial ice. Typical semi-submersibles used for exploration drilling are used as an example. The second report focus on establishing the appropriate framework to calibrate load factors for analysis of floating structures subject to loads from sea ice and glacial ice [2].

The design of the column of a typical semi-submersible was used to study the relevance of the inherent capacity to withstand a ship impact when considering impact with glacial ice. A semi-submersible is normally a mobile offshore unit and its design is governed by the maritime regulations. The study primarily focuses on the maritime regulations but also includes the requirements to how ship impact may be considered for permanent facilities. Following clarification of the regulations, the glacial ice motions are estimated using the software Wadam. In the analyses the glacial ice is limited in size to a waterline length of maximum 15 m. This size reflects the reduced possibility to detect and avoid interactions with small glacial ice pieces in waves. The glacial ice motions are used to estimate its relative displacement compared to a typical semi-submersible in order to establish the vertical extent of where ice may hit the facility. The glacial ice motions are also used to indicate the impact energies. The estimates for vertical extent and impact energy are then compared against the rules for ship impact on mobile offshore units.

The study does not consider the probability of the joint event of an interaction with glacial ice in a sea state with a given return period. Instead, it is assumed that the glacial ice will interact with the facility in selected sea states with annual probability of exceedance of 10^{-2}. The shape of the glacial ice was simplified to be either elliptical or cuboid.

An underlying assumption in the rules is that the ship impact corresponds to an impact with a vessel which mass and velocity correspond to a kinetic energy of 14 MJ. The appropriateness of using the kinetic energy of glacial ice as a method to assess the facilities capability to withstand a glacial ice impact is investigated in Chapter 8. The investigation estimates the damage from a glacial ice impact on a typical strengthened part of a semi-submersible using non-linear finite element method. Chapter 8 also applies a model used of modelling of the pressure during ice-structure interaction based on ISO 19906. This model is described, and its background is discussed briefly, in Chapter 7. Finally, in Chapter 9, the requirements to stability for mobile offshore units exposed to a ship impact is discussed in light of the applicability to use this for glacial ice impact. Identified gaps between current requirements for ship impact and the results from the study are highlighted.

2.2 Definitions

Bergy bit: a piece of glacial ice (see definition below) smaller than an iceberg but extending more than 1 m above the mean sea level. The waterline length of bergy bits is usually in the range from 5 m to 15 m.

Collision energy: see kinetic energy.

Deformation energy: the energy which must be dissipated by the body and/or the facility during an impact between the body and a facility. The deformation energy accounts for the mass and velocity the of both the free-floating body and the facility and their relative velocities.

Glacial ice: any form of ice observed at sea and originating from the deterioration and disintegration of large pieces of ice that have broken off coastal glaciers (by a process referred to as glacial calving).

Growler: a piece of glacial ice (see definition above) smaller than a bergy bit (i.e. extending no more than 1 m above the mean sea level). The waterline length of a growler is usually less than 5 m. A growler generally appears white but sometimes transparent or blue-green in colour; because of this and their relatively small size, growlers are difficult to identify when surrounded by sea ice (especially if this includes ice ridges) or when located in open water but surrounded by moderately large waves (see also WMO, 2014).

Iceberg: a large piece of glacial ice (see definition above), the height of which is at least 5 m above the mean sea level. The iceberg waterline length is generally greater than 15 m. Icebergs exhibit widely different shapes, but they may generally be described as tabular, dome-shaped, sloping, pinnacled, weathered or glacier bergs.

Impact energy: See kinetic energy.

Kinetic energy: the energy of a body, which drifts without being affected by any nearby bodies. In an interaction between a body, normally a ship, and a facility, the kinetic energy could be distributed into; translational energy, rotational energy and deformation energy.

Waterline length: the largest projected cross-sectional width of the glacial ice object, as measured in the waterline.

For general discussions of results the term "glacial ice" shall be used while results related to glacial ice of a certain mass shall be referred to by its defined term as described above.

Table 1: Categories and sizes of glacial ice after [3]. The Norwegian terms are taken from the Norwegian edition of the WMO sea ice nomenclature [4].

Category (Norwegian term)	Length [m]	Height above water [m]
Growler (knult)	< 5	< 1
Bergy bit (kalvis)	5 – 15	1 – 5
Small iceberg (lite isfjell)	15 – 60	5 – 15
Medium iceberg (mellomstort isfjell)	61 – 120	16 – 45
Large iceberg (stort isfjell)	121 – 200	46 – 75
Very large iceberg (veldig stort isfjell)	> 200	> 75

3 SHIP-IMPACT LOADS IN REGULATIONS AND STANDARDS

3.1 General

The interaction between a ship and a facility due to an accidental impact from the ship is characterized by kinetic energy, impact geometry and the indentation. Mobile offshore units operating on the Norwegian Continental Shelf are either regulated by "The Framework regulations" [5] Section 3 or the Facility Regulations [6][1], both issued by the Petroleum Safety Authority Norway. The "Facility Regulations" refer to the NORSOK Standards for design of the load-bearing structures of offshore facilities and specify the requirement to design for accidental loads as:

"Installations, systems and equipment that are included as elements in the realisation of main safety functions, cf. Section 7, shall as a minimum be designed such that dimensioning accidental loads/actions or dimensioning environmental loads/actions with an annual likelihood greater than or equal to 1×10^{-4}, shall not result in loss of a main safety function"

Section 3 in "The Framework Regulations" opens for application of maritime regulations in the offshore petroleum activities. To apply maritime regulations according to Section 3 in the "Framework Regulations", the mobile facility must be registered in a national ships' register and follow international flag state rules with supplementary classification rules providing the same level of safety as that indicated in Section 3. Section 3 specifies that the technical requirements in the Norwegian Maritime Authority's (NMA) regulations [7] for mobile facilities (red book), with supplementary classification rules provided by DNV GL, can be used.

The governing DNV GL offshore class rules for mobile offshore units are DNVGL-RU-OU-0101 [8] while DNVGL-OS-C201 [9], DNVGL-OS-C103 [10] give the structural requirements for column-stabilized units. The rig owner may also document partial compliance with verification obligations related to operation on the Norwegian continental shelf (NCS) by following DNVGL-SI-0166 [11] for assignment of the **(N)** notation.

3.2 NORSOK N-003

For permanent facilities that follow the Facility Regulations, NORSOK N-003 [12] is most relevant for assessment of ship impact on the NCS. This is usually not relevant for mobile semi-submersibles used for e.g. exploration drilling. For completeness, the requirements are included below. An updated version of NORSOK N-003 was issued in 2017 which means that the experience with the current version is limited.

3.2.1 Impact energy

NORSOK N-003 states for impact actions that:

"ALS design checks should be made with impact events corresponding to exceedance probabilities of 10^{-4}".

If no further assessment is conducted, NORSOK N-003 specifies an impact energy of:

- 50 MJ for visiting supply ships and intervention vessels

- 100 MJ for shuttle tanker collisions

---

[1] A third option follows from PSA Framework Regulations Section 24 "Use of recognized standards". Section 24 states that other solutions than those stated in PSA guidelines may be applied provided the responsible party can document that the chosen solution fulfils the regulatory requirements. Furthermore, it is stated that "maritime certificates issued by Norwegian or foreign flag state authorities, can be used as a basis to document compliance with requirements stipulated in or in pursuance of these regulations."

The effect of operational restrictions may be included in the design. For visiting supply vessels and intervention vessels NORSOK N-003 indicates the impact energy for a given maximum velocity and vessel displacement (Figure 1). A velocity of 3 m/s is a minimum unless a proven velocity limitation system is in place. Figure 1 shows that a vessel with a displacement of 10 000 tonnes drifting/travelling at 3 m/s corresponds to an impact energy of 50 MJ.
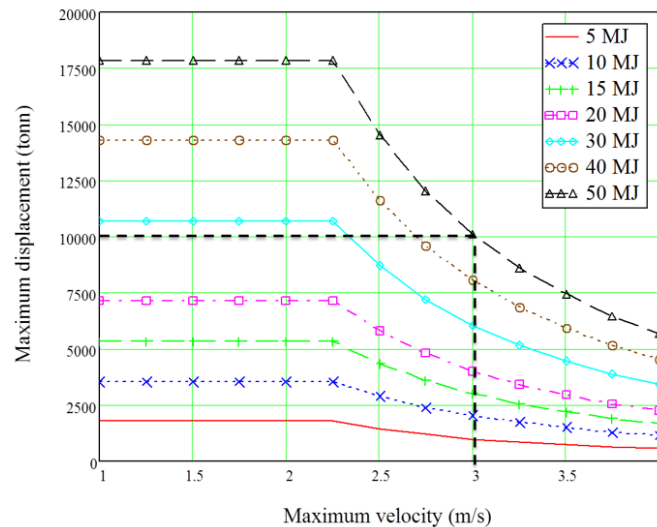
Figure 1: Operation restrictions in the safety zone (from [12])

NORSOK N-003 (2007) [13] specified for early phase design a collision energy of 11-14 MJ dependent on bow/stern or sideways collision respectively. This is specified as a ship with mass no less than 5000 tonnes, and speed of 2 m/s, added mass of 10% or 40% for bow/stern impact or sideways impact respectively.

3.2.2 Area of impact

The area of impact should be based on the dimensions and geometry of the facility and vessels operating in the area. If no further investigations are performed NORSOK N-003 [12] [13] specifies:

"the impact zone for supply vessels should be considered to between 10 m below low astronomical tide and 13 m above high astronomical tide."

3.3 Section 3 in the Facility Regulations

Mobile Offshore Units (MOU) operating on the NCS shall follow the Norwegian Maritime Authority's regulations for MOUs (red book). In addition, the flag state of the MOU may have own requirements. Most flag states acknowledge the NMA Regulations (red book) while all relevant flag states have ratified the IMO MODU Code.

Requirements to damage stability for mobile offshore drilling units because of accidental loads from ship impact are specified in:

- NMA Regulations "Stability, watertight subdivision and watertight/ weathertight closing means on mobile offshore units (12/20/1991 0878) [14]"

- IMO MODU Code Ch.3, 2009 edition [15].

The latter are adopted in the DNV GL class rules. For semi-submersibles, these are included in DNVGL-OS-C301, Ch. 2, Sec. 1, 5.4 [16].

3.3.1 Impact energy

DNVGL-OS-A101, Ch.2, Sec.1 [2.3.1] specifies that the prescriptive requirements given in CH. 2. Sec. 3 thereof, should cover the most likely hazards which may be encountered for relatively standardized designs (e.g. typical drilling units). The impact energy from a ship collision is specified as follows (A101 Ch.2 Sec. 1, [3.3.1]):

> *"The impact energy to be considered is to be based on typical size of supply vessels in the area of operation and normally not to be less than; 14 MJ (Mega Joule) for sideways collision, 11 MJ for bow or stern collision; corresponding to a supply vessel of 5000 tonnes displacement with impact speed v = 2 m/s."*

The extent of damage from the impact energy shall not lead to a horizontal penetration of more than 1.5 m within the exposed area [10]. NMA does not specify the assumed impact energy. Because the values for area of impact and the horizontal penetration is identical in NMA and IMO MODU, the 14 MJ may also be considered as the background value for the NMA regulations.

3.3.2 Area of impact

The area of impact, as illustrated in Figure 2, are being applied both by NMA and in IMO MODU/DNV GL class rules. The class rules (DNVGL-OS-C101 [17], DNVGL-OS-C103, [10]) state that:

> *"A collision between a supply vessel and a column of a column-stabilised unit shall be considered for all elements of the unit which may be exposed to sideway, bow or stern collision. The vertical extent of the collision zone shall be based on the depth and draught of the supply vessel and the relative motion between the supply vessel and the unit."*

The exposed areas are specified in DNVGL-OS-C301 as 3 m below and 5 m above the operational waterline (Figure 2).
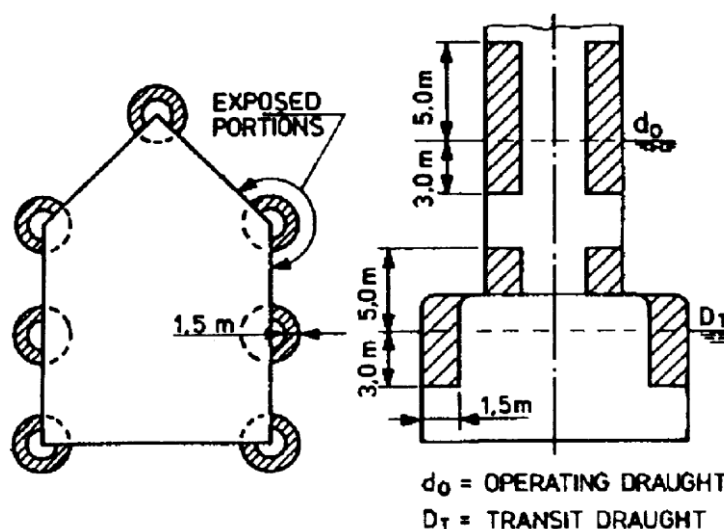
Figure 2: Exposed portions of a column stabilized unit [16].

3.3.3 N-Notation requirements

It is the owner's responsibility to ensure that the unit fulfils the requirements in the NMA regulations. To be allowed to operate on the NCS the owner must obtain an "Acknowledge of Compliance" from PSA. The Acknowledge of Compliance expresses PSAs confidence that petroleum operations can be pursued by a mobile facility in compliance with the regulations.

Partial compliance with verification obligations related to operation on the Norwegian continental shelf (NCS), can be obtained through an **(N)** notation. This can be obtained through DNVGL's voluntarily class notation **(N)** (see DNVGL-SI-0166 [11]).

PSA has imposed requirements with respect to accidental loads from ship impact on mobile offshore units which is adopted in the **(N)** (described in [11]):

- A control shall be made in the accidental limit state (ALS) with accidental loads with an annual probability of exceedance of 10^{-4}.

- Mobile facilities shall be designed to resist at least 35 MJ

Because of the PSA requirements, it has been owners' choice to mitigate the risks by imposing operational requirements to vessels servicing the units together with access area restrictions in order to keep the consequences within the initial damage criteria specified by DNVGL-OS-C301 (14 MJ).

4 GLACIAL ICE ANALYSIS

4.1 General

In order to assess the impact of glacial ice with a semi-submersible, their response to the wave environment must be established. Thus, the horizontal/vertical displacement, velocity and added mass of both bodies are to be determined. This enables calculation of kinetic energy which is comparable to impact energy used for examining impact between an offshore facility and a ship. By means of the relative vertical displacement between the glacial ice and the semi-submersible the possibility of an impact outside the part of the columns which normally is strengthened against ship impact may be assessed.

4.2 Semi-submersible

In this study a geometrical model from Genie Sesam set of user examples is used as a typical semi-submersible. Figure 3 shows the finite element model and Table 2 gives the dimensions important for the following work. Since this is a generic model, only the large volume parts of the semi-submersible are included (i.e. braces are not modelled in the model). It is assumed that the lack of detailed modelling will not affect the extreme response of the facility.
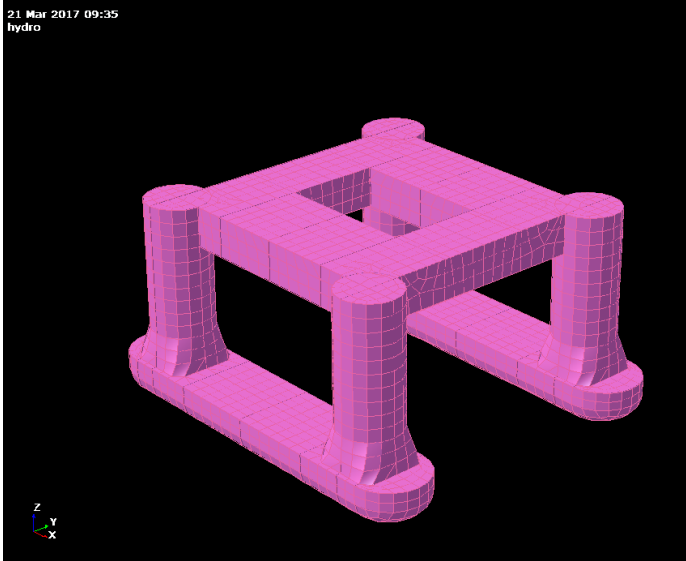
Figure 3: Panel model of the semi-submersible used in the present analysis.

Table 2: Semi-submersible dimensions.

Dimension	Size
Length of the pontoon	81 m
Width of the pontoon	16 m
Height of the pontoon	7.5 m
Distance between pontoon centers	55 m
Diameter of a column	14 m
Height of a column	34 m
Height of the deck	8 m
Draft	19.5 m
Mass	25 000 t
Metacentric height $GM_4 = GM_5$	3.51 m
Natural periods	
Heave T_3	20.8 s
Roll T_4	47 s
Pitch T_5	37 s

4.3 Glacial ice shape and mass

In this study, the glacial ice to be considered is confined to bergy bits, which range from 5 to 15 m in projected waterline length (longest dimension at the waterline). The background for assessing glacial ice of this size is the limited capability for an ice management system to detect and avoid a collision with these relatively small pieces of glacial ice [18]. Two iceberg shapes are analyzed: (a) prolate spheroid and (b) cuboid (see Figure 4). For each shape, all dimensions are defined by the ratio between the greatest horizontal axis and the dimension similar to those presented [19]. For the spherically shaped glacial ice one of the horizontal semi-axis is c, then, both the second horizontal semi-axis and the vertical semi-axis are defined as

$$a = 0.7\,c \cdot exp(-0.00124c) \tag{1}$$

Similarly, for the cuboid with length L, the height and breadth are defined as

$$H = 0.7\,L \cdot exp(-0.00124L) \tag{2}$$

$$H = B$$

The waterline for a cuboid is defined by L while $2c$ is slightly greater than the waterline length for the spheroid. Table 3 lists the dimensions for the chosen glacial ice used in the hydrodynamic analysis based assuming an ice density of 900 kg/m^3.
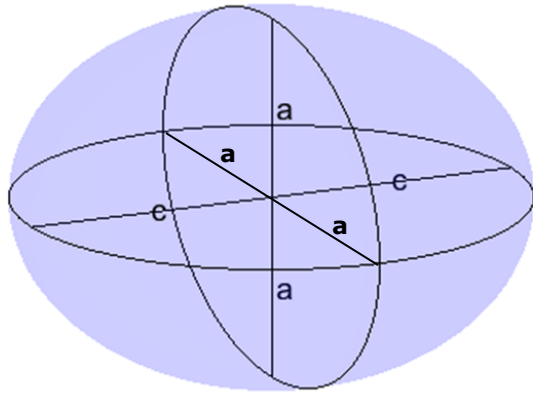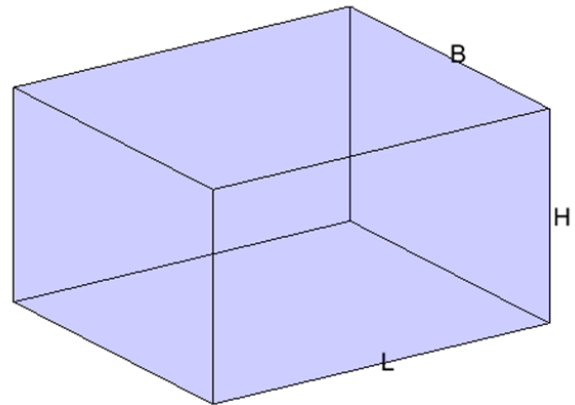
(a)   (b)

Figure 4: Glacial ice shapes: (a) - prolate spheroid, (b) - cuboid.

Table 3: Dimensions and resulting masses for each glacial ice shape and size considered in the hydrodynamic analysis.

Case	2c (=L) [m]	2a (=H) [m]	Mass [t]	Draft [m]
Spheroid				
1	5.0	3.5	29	2.7
2	12.0	8.3	390	6.5
3	15.0	10.4	765	8.1
Cuboid				
4	5.0	3.5	55	3.1
5	12.0	8.3	744	7.3
6	15.0	10.3	1432	9.0

4.4 Hydrodynamic analysis

The hydrodynamic analysis has been performed using Wadam, which is a part of the Sesam HydroD software package. Wadam is a general analysis program for calculation of wave-structure interaction for fixed and floating structures of an arbitrary shape. Both single-body and multibody analysis can be conducted within Wadam. Wadam solves a linear radiation-diffraction problem for inviscid fluids in frequency domain. One of the basic assumptions to apply the potential theory implemented in Wadam is that the flow around a body can be considered as inviscid, i.e. frictionless, and irrotational. Wadam allows to account for a degree of viscous damping which is added manually as an input to the simulation settings. This may be assessed from a stochastic analysis over a set of sea states or based on a-priory experience and/or knowledge on motions of offshore facilities. However, if the skin friction or vortex shedding effects are prevailing due to, for example, body shape characteristics, the assumption of potential theory is violated. For such cases, other analysis programs where viscous effects are modelled accurately should be considered. Also, floating bodies that experience large changes in the waterline due to the motion of the body are not well modelled within the framework of linear potential theory.

Examples include semi-submersibles in survival draft where the pontoons may come out of water in extreme waves, and small icebergs that may experience large rotations leading to large changes in the waterline. In this respect, the 'bergy bits' under 10 m of waterline have been of a concern for the given study. After careful consideration of the results for Cases 1 and 4 in Table 3 it was decided not to include them into the final report.

In a single-body analysis there is no hydrodynamic interaction between the glacial ice and the semi-submersible while in a multibody analysis the hydrodynamic pressure acting on one body is influenced by the presence of the other body. A multibody analysis is required for bodies in close proximity. Due to large difference in displaced volume, the semi-submersible is not affected by the glacial ice even for close proximity. However, as seen in Section 4.4.2, the glacial ice is influenced by the presence of the semi-submersible.

Wadam produces transfer functions of the response of the structure (also known and *Response Amplitude Operators - RAOs*), defined as response amplitude per unit wave amplitude. RAOs are generated for the 6 components of the rigid body motion: (i) three translations — surge, sway, heave and (ii) three rotations — roll, pitch and yaw, see Figure 5 for definition. The response spectrum of the motion in a particular irregular sea state, characterized by significant wave height Hs, spectral peak period Tp and wave spectral shape (wave spectrum) may be found by combining the wave spectrum with the relevant motion RAOs in the frequency domain. The RAOs can also be combined to, for example, evaluate the displacement of a point located on the body in vertical and/or horizontal direction.

Viscous damping is added as a percentage of the critical damping in the present analysis. The critical damping characterises a system that does not develop any oscillations after an excitation and quickly returns to its steady state. The critical damping coefficient is defined as

$$c = 2\sqrt{km}$$

where k is the stiffness of the system and m is its mass. The applied damping levels for heave, roll and pitch modes specified in Section 4.4.2 are set based on experience with semi-submersible motions and by evaluating the motion RAOs of the single body analysis of the glacial ice shapes.
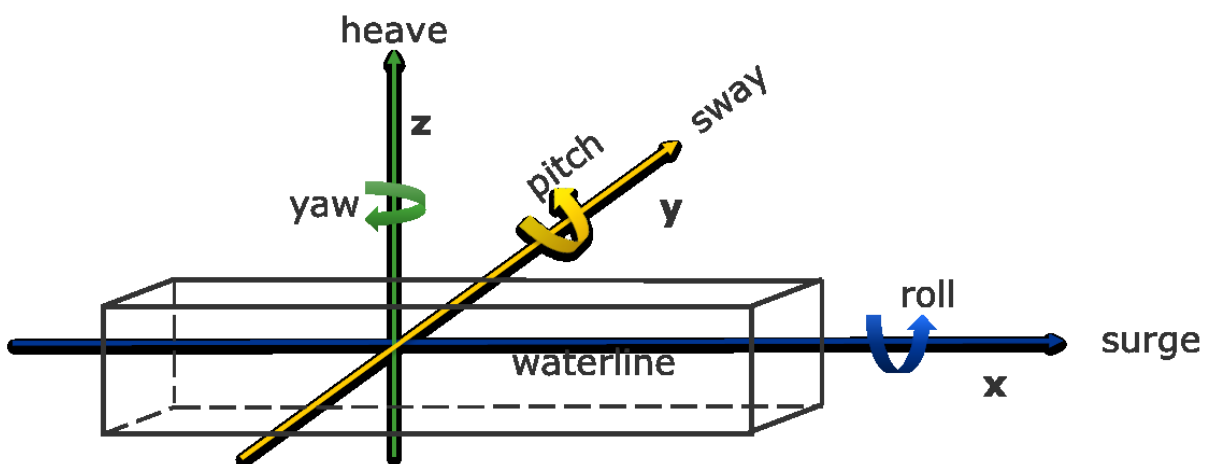

Figure 5: Six basic components of rigid body motion.

An objective of the analysis is to identify the vertical extent of a semi-submersible which is exposed to glacial ice impact. Thus, the motion components which add to the vertical displacement are of main

interest, namely, heave, pitch and roll. Since both the glacial ice and facility are floating, their relative vertical displacement requires the response of both bodies. Both single-body and multibody analysis are used to investigate possible hydrodynamic interaction effects, and the resulting RAOs are presented in Section 4.4.2. The second objective is to estimate kinetic energy of the glacial ice. This is determined by establishing horizontal velocity, body and added mass for each piece of glacial ice. The added mass, a quantification of the water moving with the ice, is in this case found by considering the effect of horizontal motion only. To identify the medium and 90 % quantile values for displacement, velocities and kinetic energy the statistical postprocessing presented in Section 4.4.4 is used; the results are presented in Section 5.

4.4.1 Wave spectrum and sea states

The JONSWAP wave spectrum, see for example DNVGL-RP-C205 [20], is used for the analysis. The JONSWAP wave spectrum is characterized by significant wave height Hs, spectral peak period and a peak shape factor. The sea states in the present work were chosen on the Hs-Tp contour corresponding to the 100-year return period from the location 74.00˚N, 35.67˚E (Figure 6). The three pairs listed in Table 4 are used in the following analysis and were chosen to illustrate some of the variation in the outcome along the 100-year return period contour. Typically, when selecting sea states along a contour line the peak of the contour is selected. In addition, two sea states with Tp lower than peak of the contour is selected for the present study. For the glacial ice of medium size (case 2 and 5) the natural period in heave is approx. 6.5 s motivating a peak period of 6.5 s. With reference to Figure 25 it is seen that a sea state with Tp around 8 s is also an interesting sea state for the large cuboid (but has not been analysed). Figure 7 demonstrates the resulting JONSWAP wave spectra. The peak shape factor is based on the formulation given in DNVGL-RP-C205 and is a function of Hs and Tp.
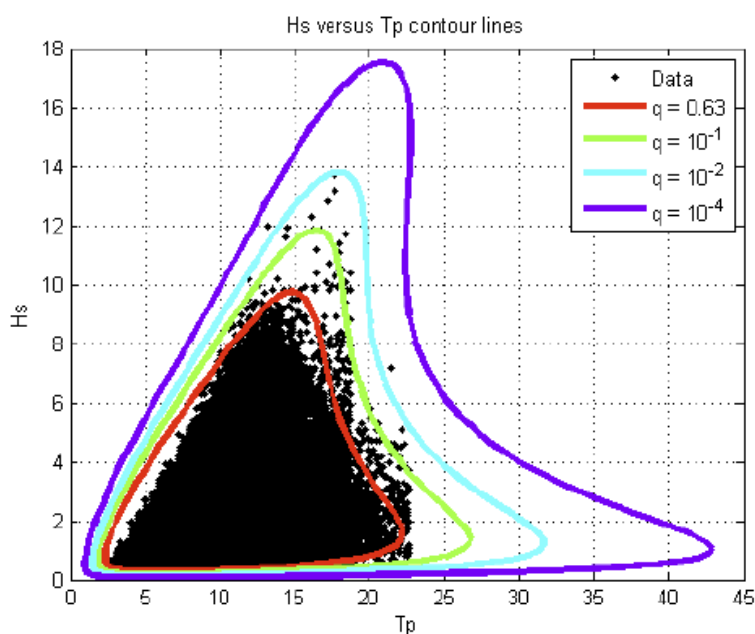

Figure 6: The Hs-Tp contour lines which is used as basis for the current study (after [19]).

Table 4: Sea states considered in the analysis.

Sea state	Tp	fp	Hs	γ[1]
	[s]	[Hz]	[m]	[-]
1	6.5	0.15	6	5.0
2	14	0.07	12	3.0
3	18	0.06	13.8	1.2

Notes: [1]Peak shape factor
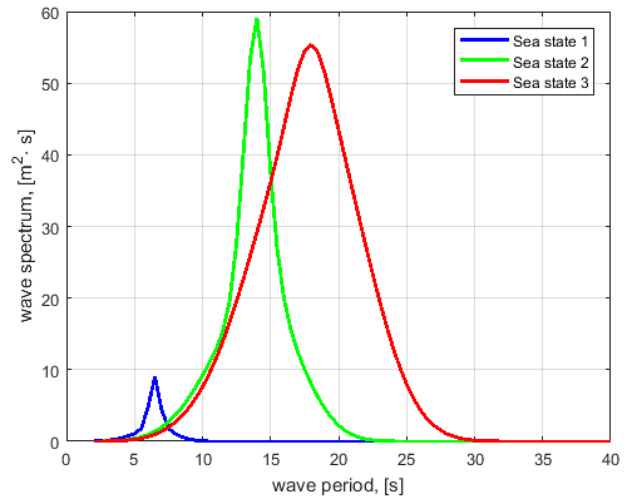
**Figure 7: JONSWAP wave spectrum with respect to wave period for different sea states.**

4.4.2 RAOs for semi-submersible and glacial ice

The response amplitude operators (RAOs) corresponding to heave, $\eta_3(\omega,\beta)$, roll, $\eta_4(\omega,\beta)$, and pitch, $\eta_5(\omega,\beta)$[2], of the glacial ice and the semi-submersible resulting from single-body and multibody analysis are presented. For illustrative purposes the discussion is limited to case 3 and 6 in Table 3, i.e. the largest glacial ice shapes. The position of the two bodies loaded into the multibody analysis is presented in Figure 8. Note, that the RAOs are given in the body coordinate system; the global coordinate system coincides with the coordinate system attached to the semi-submersible. The wave direction in the analysis is 270° counter clockwise to positive direction of the x-axis (beam seas); that results in a movement of the glacial ice towards the semi-submersible.

As it was mentioned above, the additional damping due to viscous effects should be added as an input to the Wadam analysis. For the given study, the level of critical damping added for the glacial ice in heave, roll and pitch is 7 %, 11 %, and 11 %, respectively; for the semi-submersible, it is 5 %, 7 % and 7 %. Especially the damping level for the glacial ice shapes are uncertain and the damping levels are selected such that unrealistic large motions close to the natural periods are depressed. This is a topic for further research and assessment of drag and damping are part of scope of work in the planned joint industry project (JIP) 'Glacial Ice Impact Loads on Floaters'. The JIP will be executed by DNV GL and C-Core and is planned to start in 2018.

---

[2] The RAOs are a function of wave frequency ω and wave direction β.
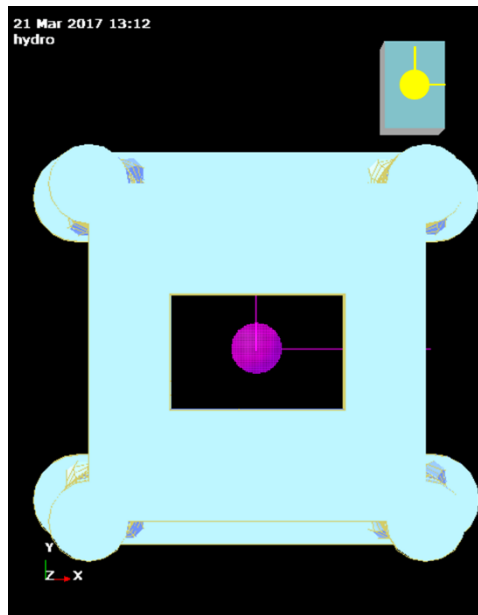
Figure 8: Relative position of the glacial ice and semi-submersible for multibody analysis. The magenta and yellow circles indicate the motion reference points for the RAOs.

The RAOs corresponding to heave, roll and sway for wave periods between 1 s and 40 s are shown in Figure 9 for the semi-submersible. The semi-submersible is neither influenced significantly by the presence nor the shape of the glacial ice when it is close to the semi-submersible.

Figure 10 demonstrates the response of the glacial ice in heave, roll and sway for both spheroid- and cuboid-shaped ice. As ice masses for these shapes are much smaller than the mass of the semi-submersible, the glacial ice is affected by the presence of the semi-submersible. The effect on the spheroid is similar to the effect on the cuboid, and pronounced differences are observed, in particular, for the roll motion where the maximum response for the multibody analysis is approx. 30 % lower than the response in the uncoupled analysis. Also, it is seen that the roll motion for the spheroid has two peaks while there is only one peak for the cuboid. For the spheroid, the natural period in roll is 11 s and the eigen solutions show that coupling effects between the different modes are very small.

From the wave excitation forces for the spheroid, it is seen that the heave excitation force has a peak at approx. T = 4 s. This peak, that is not present for the cuboid, can be explained by the shape of the spheroid and its deep draft leading to a hydrodynamic pressure both on the lower and upper part of the spheroid. Hence, the peak at 5 s for roll is most likely due to a coupling between heave and roll and is not related to the natural periods of the spheroid.

For the two smallest ice shapes a larger influence from the semi-submersible is expected. The motion RAOs show that there are important differences between single- and multibody hydrodynamic analyses for wave frequencies where the wave spectrum has its main energy.
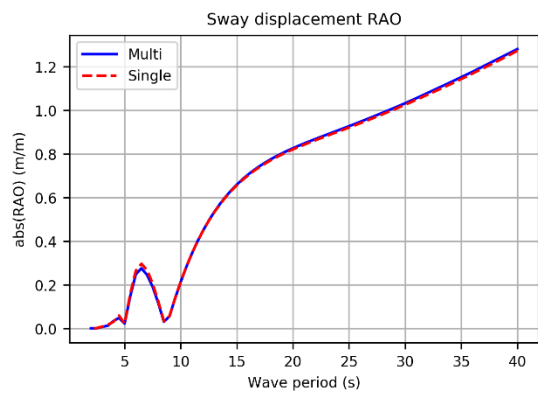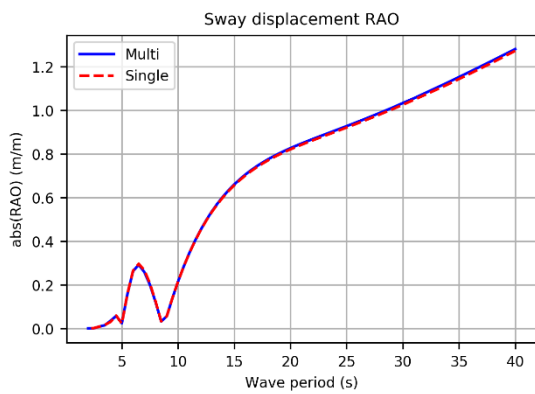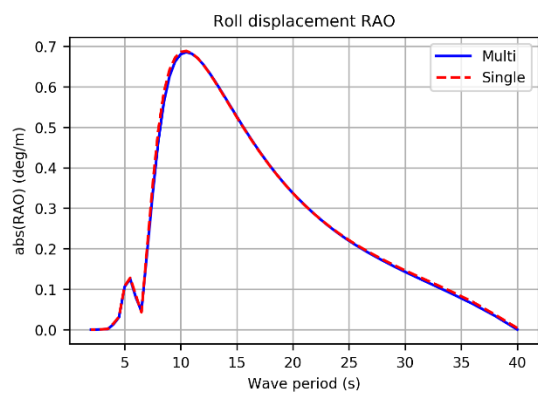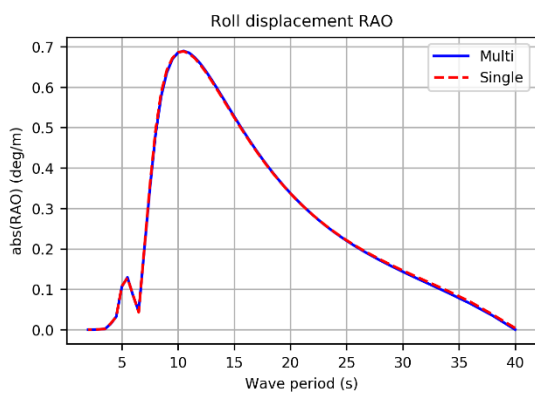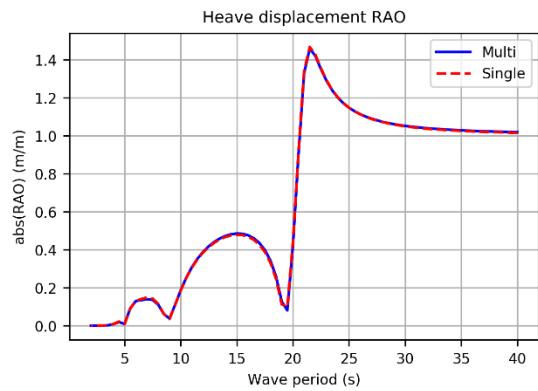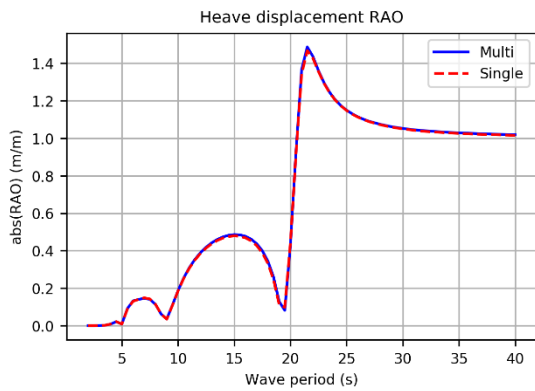
Figure 9: The response of the semi-submersible in (from top to bottom) heave, roll and sway from a single and multibody body analysis with (a) — spheroid and (b) — cuboid. Wave direction 270 deg.
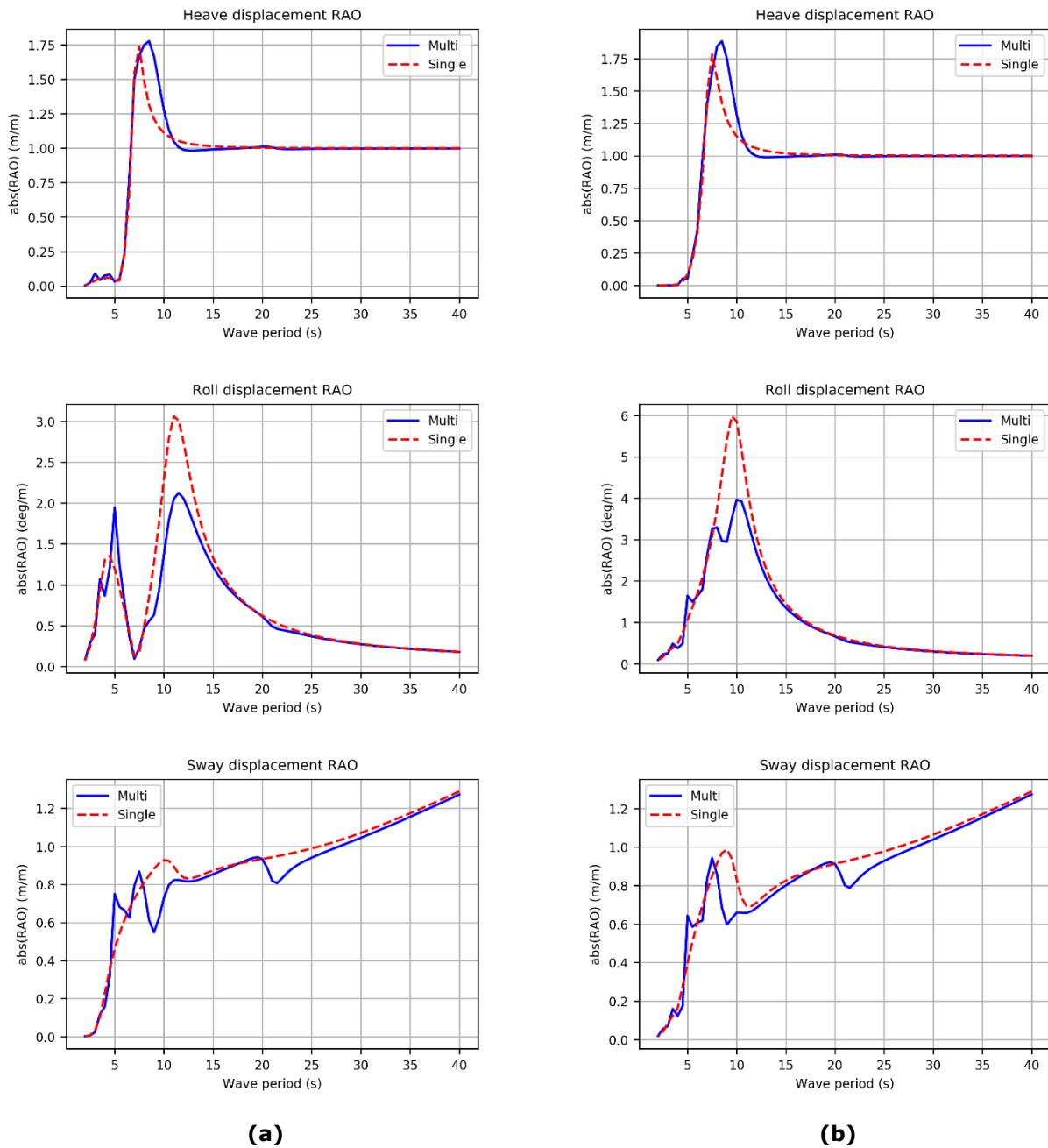
Figure 10: The response of the glacial ice in (from top to bottom) heave, roll and pitch from a single and multibody body analysis for spheroid − (a) and cuboid − (b). Wave direction 270 deg

4.4.3 Relative vertical displacement

A vertical displacement RAO of a body at point $p = (x_p, y_p, z_p)$ is derived as combination of RAOs for heave, $\eta_3(\omega, \beta)$, roll, $\eta_4(\omega, \beta)$, and pitch $\eta_5(\omega, \beta)$ as

$$VD(\omega, \beta) = \eta_3(\omega, \beta) - x_p \sin[\eta_5(\omega, \beta)] + y_p \sin[\eta_4(\omega, \beta)] \tag{3}$$

where ω is angular frequency (rad/s) and β is the wave direction in degrees, for details see reference [21]. If $VD_i(\omega, \beta)$ and $VD_s(\omega, \beta)$ are RAOs for vertical displacements of the glacial ice and semi-submersible, then their relative displacement is derived by

$$RD(\omega, \beta) = abs\big(VD_i(\omega, \beta) - VD_s(\omega, \beta)\big) \qquad \textbf{(4)}$$

The location of point $p = (x_p, y_p, z_p)$ is illustrated in Figure 11, and relevant values for all cases are presented in Table 5. The resulting RAO for the relative vertical displacement (at point p) for Case 3 and 4 (Table 3) both for single- and multibody analysis are demonstrated in Figure 12. The peaks of the relative vertical displacement are located at the roll and heave natural periods of the glacial ice and the semi-submersible (about 7 and 20 s for Cases 3 and 6). For further analysis, the sea state modal frequencies are also chosen near these peaks. The relative horizontal velocity (sway) for wave direction 270° (at point p) is shown in Figure 13 for single- and multibody analysis for the large glacial ice shapes. Differences are observed for peak periods lower than 15 s and there is also a small coupling effect with the natural period in heave around 20 s.

It is emphasized that the relative vertical displacement and horizontal velocity is not calculated at the time of impact.
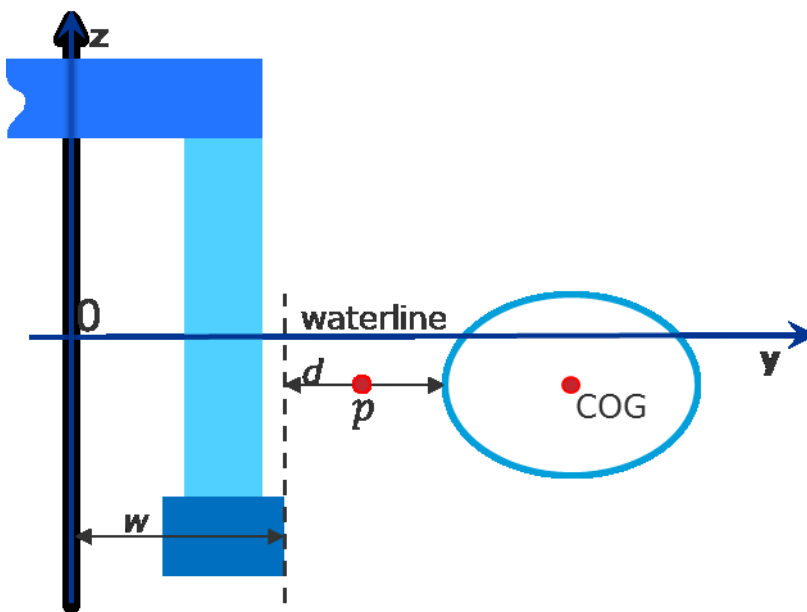
$COG = (x_{COG}, y_{COG}, z_{COG})$ - centre of gravity of glacial ice in global coordinate system;

$d = 2.76\, m$ - distance in y-direction between pontoon and leading edge of the glacial ice;

$w = 35.5\, m$ – distance from the middle of the semi-submersible to the outer side of the pontoon,

$p = (x_p, y_p, z_p)$ - reference point, where

$$x_p = x_{COG}$$

$$y_p = w + d/2$$

$$z_p = z_{COG}$$

Figure 11: Definition of the reference point p for calculation of the relative vertical displacement.

Table 5: Centre of gravity of glacial ice in global coordinate system.

	x_{COG} [m]	y_{COG} [m]	z_{COG} [m]
Case 1	27.4	40.8	-1.0
Case 2	27.4	44.3	-2.3
Case 3	27.4	45.8	-2.9
Case 4	27.4	40.8	-1.3
Case 5	27.4	44.3	-3.1
Case 6	27.4	45.8	-3.9
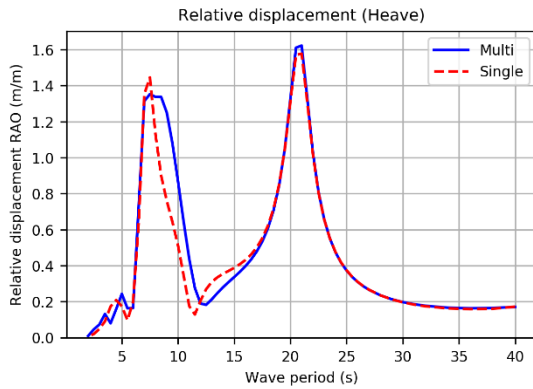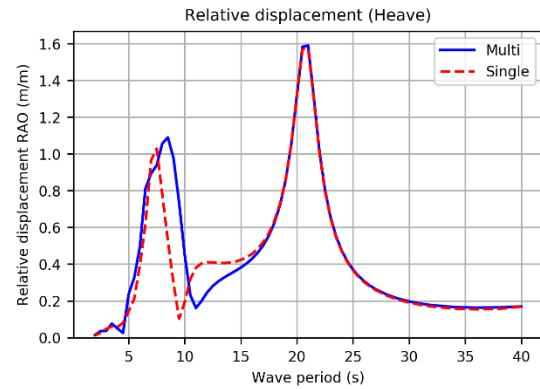
(a)　　　　　　　　　　　**(b)**

Figure 12: RAOs of relative vertical displacement for the glacial ice and semi-submersible from single- and multibody analysis for spheroid − (a) and cuboid − (b)
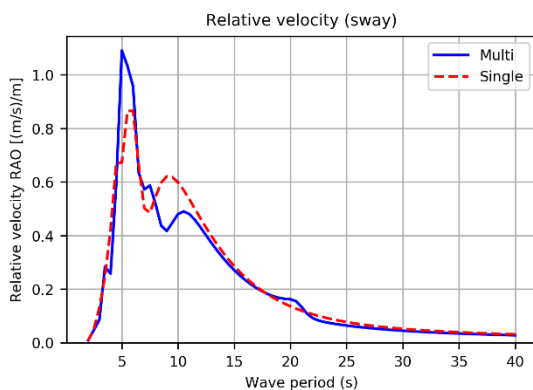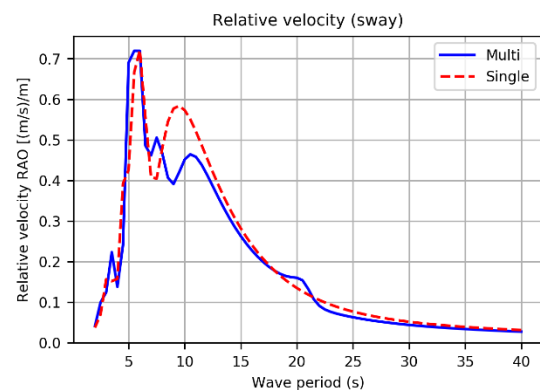
(a)　　　　　　　　　　　**(b)**

Figure 13: RAOs of relative horizontal velocity (sway) for the glacial ice and semi-submersible from single- and multibody analysis for spheroid − (a) and cuboid − (b)

4.4.4 Postprocessing

To estimate the area of impact, velocity and added mass to be used in energy estimations, the statistical theory of narrow-banded processes [22] is applied in this study. The basic assumption for a narrow-banded process is that all the maxima are positive-valued (and all the minima are negative valued). The path, also called *cycle*, of such process from a local minimum to a consequent local maximum would cross the zero-line only once. Thus, the distribution of the peaks can be determined from the frequency of zero-crossings. Further, since the response of a freely floating body in irregular waves is Gaussian distributed, it can be shown that if assuming a narrow-banded process, the response peaks are Rayleigh distributed with the probability density function

$$f(z) = \frac{z}{\sigma^2} \exp\left(-\frac{z^2}{2\sigma^2}\right) \tag{5}$$

where the standard deviation is σ. The zero up-crossing frequency f_0 for a certain duration is defined as $f_0 = \frac{1}{2\pi}\sqrt{\frac{m_2}{m_0}}$ with spectral moments $m_n = \int_0^\infty \omega^n W(\omega)\,\mathrm{d}\omega$, where $W(\omega)$ is the spectral density function (spectrum) of the process. Also, the standard deviation is related to the zeroth spectral moment by $\sigma = \sqrt{m_0}$. The added mass used for the energy estimation corresponds to the period of zero up-crossings for each sea state, namely at $T_0 = f_0^{-1} = 2\pi\sqrt{\frac{m_0}{m_2}}$. Here the moments are calculated for the wave spectrum $S(\omega, \beta)$.

The relative vertical displacement between the glacial ice and the semi-submersible can be described by a single response spectral density function. By using this response spectral density function the median and 90 % quantile displacement values for the relative displacement of the two bodies are estimated using Eq. (5). Similarly, velocity values are also estimated using Eq. (5) with the spectral density function of velocity response.

Assuming a stationary sea state with N independent local maxima, for example, wave crest heights, with a cumulative distribution function $F(x)$, the distribution of the extreme maximum is given as $F_E(x) = F(x)^N$ which is also referred to as the extreme value distribution. As discussed, the local maxima are assumed to be Rayleigh distributed, and the extreme maximum x_E is given by

$$x_E(p) = \sigma\sqrt{-2\ln(1 - p^{1/N})} \tag{6}$$

where the quantile level is given by p. The extremes will be calculated for a duration of three hours, i.e. $N = 10800/T_0$. When the response is calculated from RAOs $H(\omega, \beta)$ and a wave spectrum $S(\omega, \beta)$, the spectral moments are defined as

$$m_n = \int_{-\pi}^{\pi}\int_0^\infty \omega^n |H(\omega, \beta)|^2 S(\omega, \beta)\mathrm{d}\omega\mathrm{d}\beta \tag{7}$$

As before, the standard deviation and zero-crossing period of the response are given by $\sigma = \sqrt{m_0}$ and $T_0 = \frac{1}{2\pi}\sqrt{\frac{m_2}{m_0}}$, respectively. An illustration of the distribution of local maxima and the extreme value distribution is shown in Figure 14, and details regarding the estimation of the extremes can be found in DNVGL-RP-C205 [20].
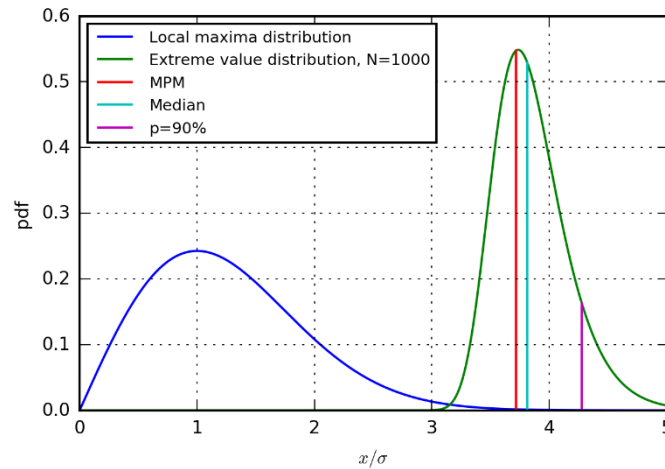
Figure 14: Example of the local maxima distribution (Rayleigh) and the extreme value distribution. Also included is the most probable maximum (MPM), the median and the 90 % quantile value.

4.5 Non-linear motion response of glacial ice

The Wadam analysis presented in Section 4.4 is based on linear potential theory. To address non-linear effects the largest spheroid is selected for further analysis with Wasim [23]. The reason for choosing the spheroid is that for this geometry, the water plane area changes significantly during one wave cycle, and this effect is not captured by the Wadam analysis which assumes a constant water plane area.

Wasim is a program for computing local loads and global response of floaters moving with forward speed. The simulations are carried out in time domain, but results can be transformed to frequency domain by using Fourier transform. Wasim solves the fully 3-dimensional linear radiation/diffraction problem by a Rankine panel method. The method requires panels both on the floater and on the free surface. In addition, several non-linear effects are included in Wasim, such as:

- Integration of hydrostatic pressure and Froude-Krylov wave pressure over the exact wetted surface.

- Quadratic terms in the Bernoulli equation are included.

- Exact treatment of rotation angles in inertia and gravity terms.

- Quadratic roll damping.

The present analysis focuses on the glacial shape only, i.e. the semi-submersible is not present. Long-crested waves are assumed, propagating along the main axis of the spheroid (surge direction). Due to symmetry of the problem, only response in surge, heave and pitch is analysed (sway, roll and yaw motions are fixed in the analysis). Analysis of regular and irregular waves are included in the present study.

4.5.1 Analysis setup

For this analysis, the largest spheroid is selected and the geometry, mass properties and the level of viscous damping are identical to the one used in the Wadam analysis, refer to Section 4.3 and 4.4.2 for details. Due to the mesh requirements in Wasim the spheroid is re-meshed and the mesh of the spheroid and free surface is shown in Figure 15. The model is also checked to ensure that buoyancy and gravity forces are in balance. Figure 16 shows the equilibrium test in calm water. For the heave motion, there

are some very small oscillations and the equilibrium position is shifted approximately 4 mm downwards meaning that the model is well balanced. A minor imbalance in mass and buoyancy is the reason for the oscillations seen in Figure 16.
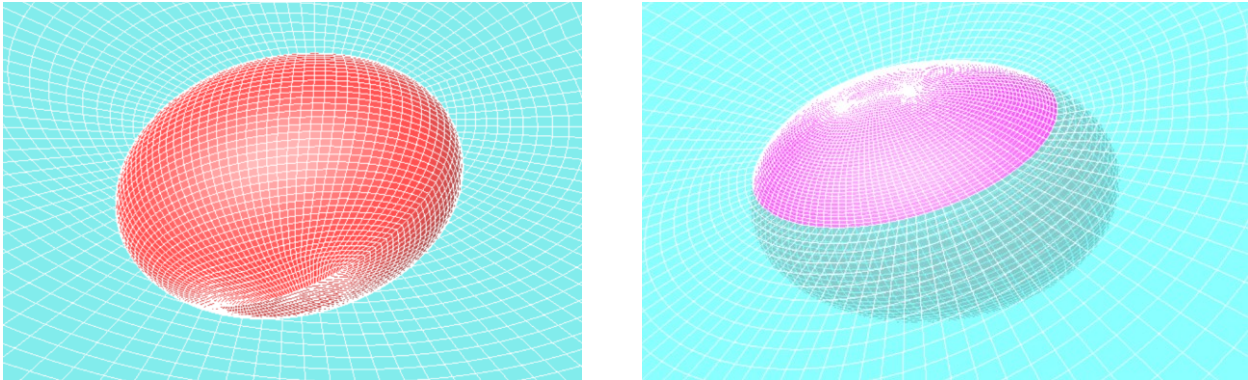

Figure 15: Mesh of large spheroid used in the Wasim analysis; wet (left) and dry (right) part of the spheroid. The free surface mesh is also included.
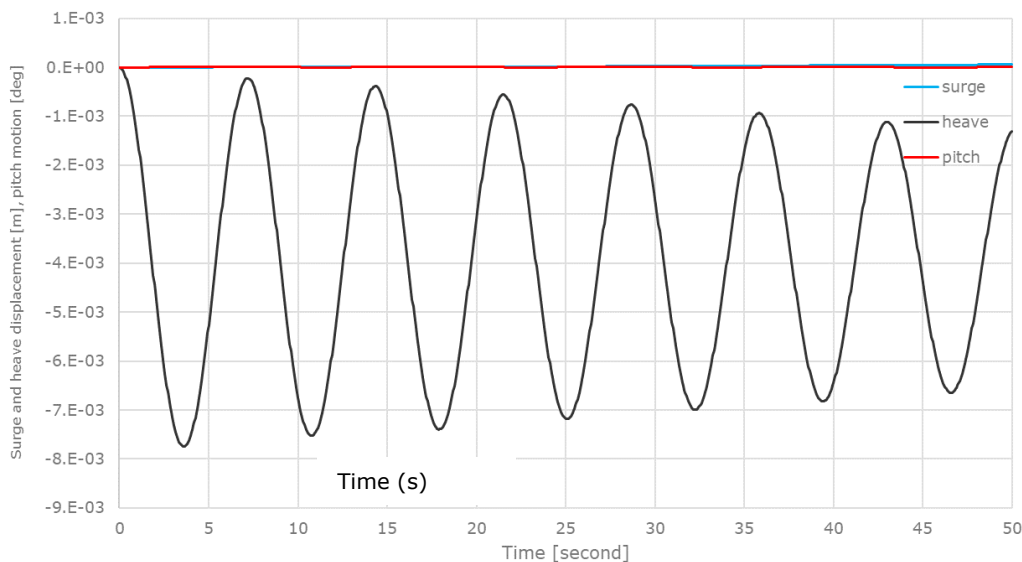

Figure 16: Calm water equilibrium position. The oscillating curve is the heave motion and the curves at zero are surge and pitch motion.

4.5.2 Linear motion response

In order to verify the Wasim model, a linear analysis (excluding the non-linear effects) is carried out and the motion time series are transformed to the frequency domain by using Fourier transforms. Hence, the motion RAOs can be compared with Wadam results. RAOs for surge, heave and pitch are presented in Figure 17 to Figure 19. The centre of gravity (COG) is chosen as the motion reference point. For heave, the RAOs are also shown for different wave headings and it is observed that the heave RAOs are almost independent of the wave heading. As can be seen from the figures, only very small differences are observed.
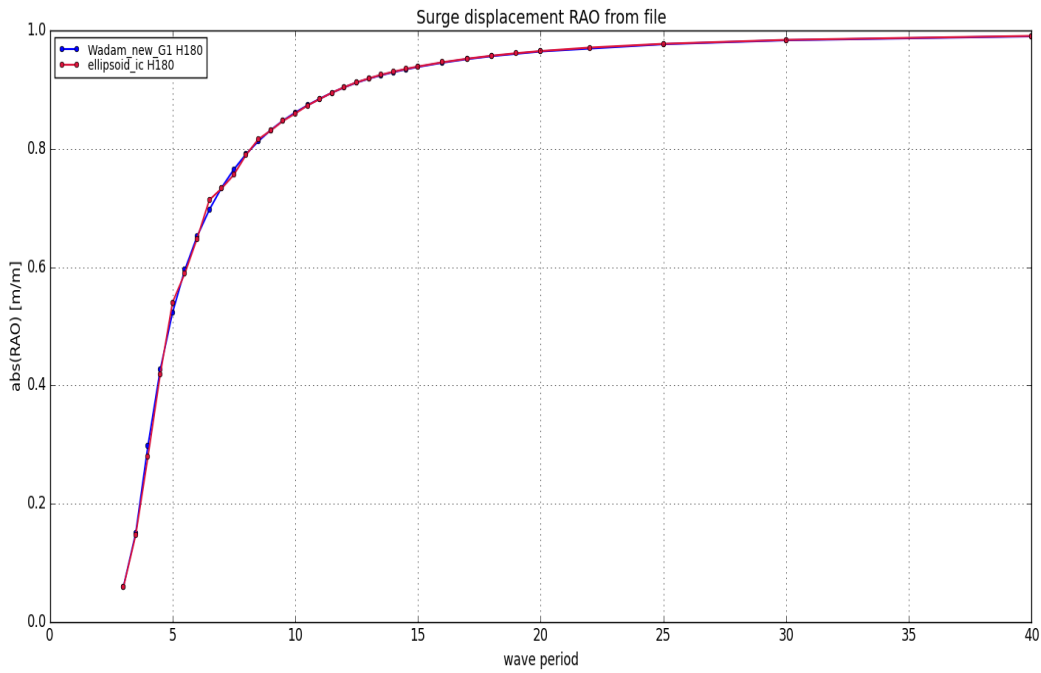
Figure 17: Surge displacement RAO; Wasim (red curve) and Wadam (blue curve).
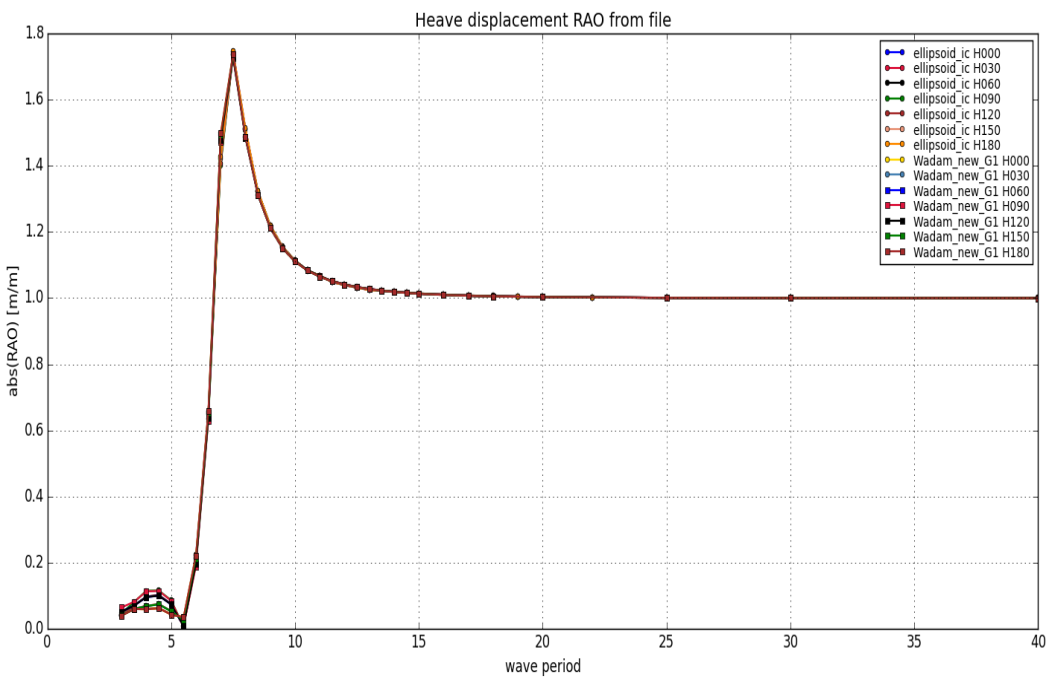
Figure 18: Heave displacement RAO; Wasim and Wadam.
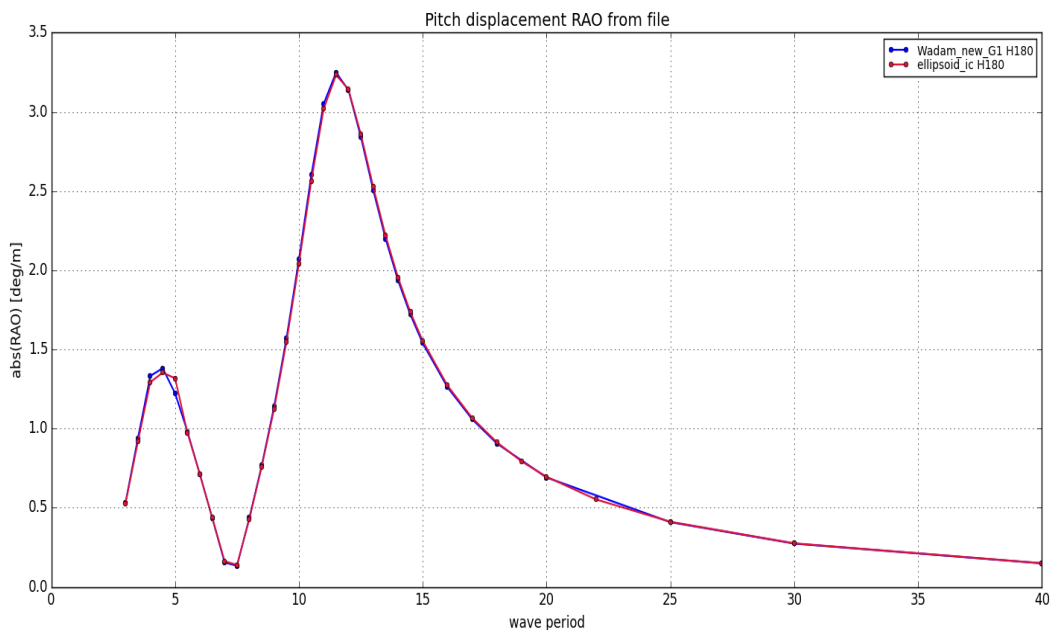
**Figure 19: Pitch displacement RAO; Wasim (red curve) and Wadam (blue curve).**

4.5.3 Linear and non-linear response in regular waves

The first non-linear Wasim analysis assumes regular waves and the results are compared with linear Wasim results. For the first analysis, the wave period is fixed at the spheroid's pitch resonant period of 11.5 s and the wave amplitude is varied between 1.5 m and 5 m. An additional analysis has been run with a wave amplitude of 6 m and a wave period of 16.2 s. The latter wave period is motivated by converting the 100-year sea state with peak period of 18 s to a regular design wave with a period of 0.9 times the peak period. Reference is made to [13].

Results for surge, heave and pitch are given in Figure 20 and Figure 21 (close-up of surge and heave). Generally, it is seen that the motion response is larger for the non-linear analysis than the linear. The reason that the maximum wave amplitude is 5 m for the case with wave period of 16.2 s is that simulations for larger wave amplitudes resulted in non-harmonic motion. For the large wave amplitudes, it was observed that the spheroid could be completely submerged and the spheroid was rotating 180 and 360 deg in pitch. Even though Wasim handles a complete submerged body the radiation and diffraction solutions are based on linear wave theory and for the initial dry part of the spheroid only Froude-Krylov forces are applied. Such situations are beyond the validity of Wasim and the results are therefore not included.

For the additional regular wave case with wave amplitude of 6 m and wave period of 16.2 s, the pitch motions are much lower than the case with wave amplitude of 5 m and period of 11.5 s due to the wave period is not at the pitch resonant period.

Figure 20 and Figure 21 show the response based on the positive amplitude of motions. Similar results can be extracted by post-processing the negative amplitudes. For the linear Wasim analysis assuming a harmonic motion, the results due to the negative motion amplitudes are equal to the response based on the positive motion amplitudes (except for the sign). Looking at the response due to the non-linear Wasim analysis, there are some differences. In particular, the pitch motion amplitudes are different based on positive or negative wave amplitudes, refer to Figure 22. The figure also shows the non-linear surge and heave motions and no differences are observed due to positive or negative amplitude of motion.
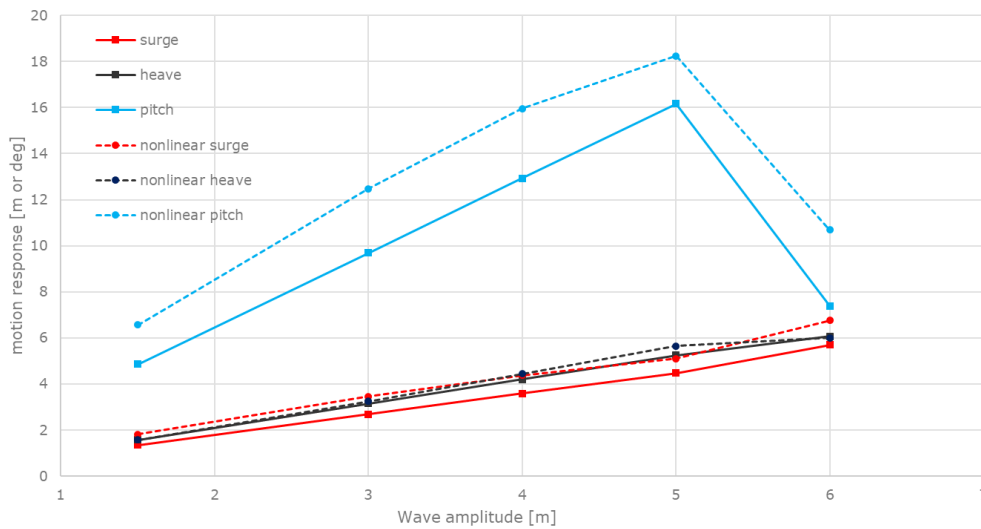
Figure 20: Linear and non-linear motion amplitude in regular waves for surge (m), heave (m) and pitch (deg). The motions are taken at COG.
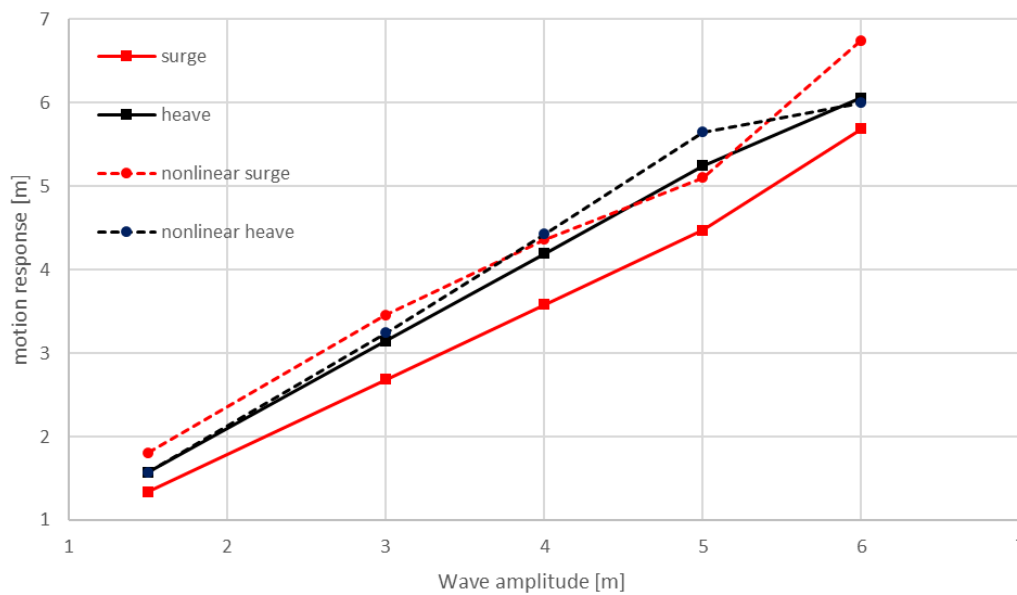
Figure 21: Linear and non-linear motion amplitude in regular waves. Close-up of surge and heave, refer to Figure 20 which also includes the heave motion. The motions are taken at COG.
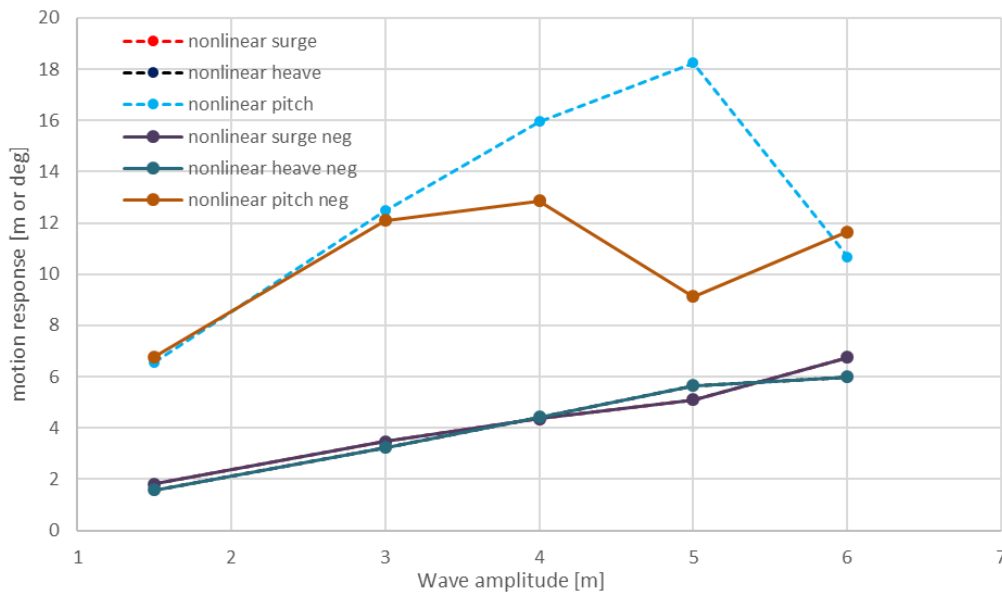
Figure 22: Comparison of positive and negative non-linear motion amplitudes (absolute values) in regular waves. On this scale, it is not possible to distinguish the results for surge and heave.

4.5.4 Non-linear response in irregular waves

The three different sea states along the 100-year Hs-Tp contour, refer to Section 4.4.1, have also been analysed with the non-linear Wasim. The simulation length of each sea state is 3 hours. A three parameter Weibull distribution is fitted to the response time series and the most probable maximum (and minimum) is estimated from the fitted distribution. Results are tabulated in Table 7 together with linear Wasim results. For the surge velocity, due to the non-linear analysis, the positive and negative velocity are approximately equal and it is also seen that the surge velocity from the linear analysis is substantial lower than the non-linear velocity. The heave motion shows a larger asymmetry for the upward and downward motions and from the numbers it is clear that the spheroid will be completely submerged for all sea states. As stated in the previous section, the validity of the Wasim results are questionable when the spheroid is completely submerged. For the upward heave motion, it is also seen that the linear response is lower than the response from the non-linear analysis.

Table 6: 3-hour most probable maximum response of large spheroid due to linear and non-linear Wasim for sea states along the 100-year Hs-Tp contour line.

Hs (m)	Tp (s)	γ	Surge velocity (m/s)			Heave (m)		
			NL+	NL-	Linear	NL+	NL-	Linear
6	6.5	5	5.8	-5.8	3.7	5.5	-15.8	4.5
12	14	3	8.8	-8.3	5.2	12.8	-28.1	11.7
13.8	18	1.2	7.3	-7.9	5.1	14.7	-31.3	12.9

Notes:
NL+ and NL- refer to non-linear Wasim results in positive and negative direction, respectively.

4.5.5 Summary of non-linear time domain analysis

Time domain simulations with the program Wasim are carried out for the large spheroid. For verification purposes, it is demonstrated that the spheroid is in equilibrium in calm water and motion RAOs from Wasim and Wadam simulations are compared and shown to be equal.

Motions calculated by non-linear Wasim are larger than motions calculated by linear Wasim in regular waves. Heave motion amplitudes have similar amplitudes in the linear and non-linear simulations, surge motion amplitudes differ more, while there are large differences for pitch.

To obtain more stable non-linear Wasim simulations, pitch stability should be increased to avoid overturning. In the current simulations, pitch GM is only 0.55 m. In the non-linear Wasim 3-hour simulations, pitch motion time series show full turns (at 360, 720, 1440 and 1800 degrees' pitch motion) and half turn (with top down at 540 degrees' pitch motion). Another aspect for the cases where the glacial ice is rotating full turns, is that the large motions will result in increased viscous damping which will have a stabilizing effect.

In the current simulations, sway, roll and yaw motions are fixed. If the roll motion is to be simulated, roll stability is even smaller (GM is only 0.0054 m) and this will no doubt affect accuracy of the non-linear simulations for the case when the body is topside down.

Non-linear Wasim simulations indicate higher kinetic energy for free floating glacial ice. Table 6 shows that the horizontal velocity from non-linear analysis is about 50% higher than results from linear analysis. This translates to an increase in kinetic energy of 120-170%. It is pointed out that Wasim is a single body program and cannot analyse a multi-body configuration.

5 GLACIAL ICE IMPACT

5.1 Area of impact

All facilities operating on the Norwegian Continental Shelf are designed to withstand an impact with a ship. Unless further evaluations are performed the exposed areas to damage for a mobile offshore unit are 3 m below and 5 m above the operational waterline (see Section 3 for details).

The estimated area of impact is based on the relative vertical displacement between the glacial ice and the semi-submersible in point p as illustrated in Figure 11. The analysis is based on a multibody analysis. Point p is located at the depth of centre of gravity of the glacial ice and its location between the two bodies is given in Table 5.

For the spheroid shaped glacial ice, the first point of contact on the glacial ice is assumed to be the tip of the glacial ice. The tip, indicated by the red dot in Figure 23(a), is used as the reference point in the present analysis and is at the same depth as the body's centre of gravity. Unlike spheroid shaped glacial ice, cuboid shaped glacial ice have a shape that implicate a greater variation in which part of the shape that may impact the facility. The contact point could vary between the upper and lower corner of the cuboid, shown as grey points in Figure 23(b). In the present analysis, the reference point for the cuboid shaped glacial ice is at the same depth as the centre of gravity (red dot in Figure 23(b)).

The analysis investigates the vertical offset between the facility and the glacial ice body at the reference depth (Table 7). An offset of ±1 m for a spheroid with reference depth of -3 m suggests that the glacial ice will hit the facility at depths between -4 m and −2 m (-3 m ±1 m).
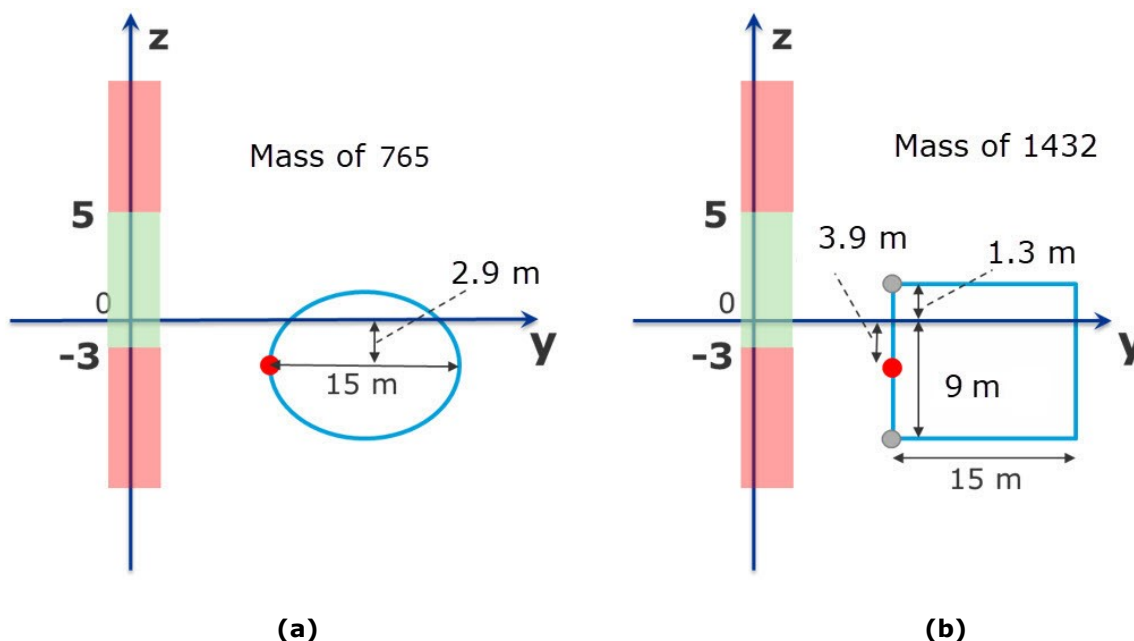
Figure 23: Illustration of the elevation of the reference points used to assess the impact point, Cases 3 and 6 are shown.

The density of glacial ice is about 10 % lower than that of sea water. This means that most of the body of the glacial ice is below the waterline. The reference elevation for the investigated shapes and sizes range from 2.3 m to 3.9 m below the waterline (Table 7). This is at or below the depth for which columns must be designed to withstand a ship impact.

The result of the analysis of vertical impact elevations are given in Table 7. The vertical impact elevations associated with probability of non-exceedance of 50 % and 90 % are estimated per sea state, glacial ice shape and size. The values and the respective probability can be considered as the probability for the value not being exceeded in a 3-hour storm period. The method is described in Section 4.4.4 and follows that of DNVGL-RP-C205 [20]. An illustration of the distribution of the local maxima and the extreme value distribution is shown in Figure 14.

The analysis shows that the lower impact extent could be as low as -14 m which is significantly lower than the draft of the top of the pontoon which is at -12 m (Table 7). All cases show that the glacial ice may impact on the pontoons.

To get an indication of the effect of the severity of the sea state, in terms of return period, a sensitivity study using the largest cuboid is carried out. Return periods of 1 and 10 years are selected in addition to the 100-year return period which is the base case. The selection of sea states includes the peak wave height and two additional sea states with lower peak periods and wave heights. Table 8 and Figure 24 show the relative vertical impact elevation and horizontal velocity (sway) between the large cuboid and the semi-submersible for the selected sea states. The results show that the maximum relative vertical displacement occurs for the sea state at the peak of the Hs-Tp contours (see Figure 6) and the response is decreasing for decreasing wave height (Hs), as expected. For the relative velocity, the maximum relative velocity does not occur at the peak of the contour but at slightly lower periods. From Figure 25, the relative velocity per unit wave height is decreasing with increasing peak period. However, this effect is not readily visible in Table 8 as the wave height increases with increasing peak period. From Figure 24 it is also seen that the effect of reducing the return periods is much more pronounced for the relative vertical motion than for the relative velocity.

For sea state 3 (Hs = 13.8 m) both shapes of glacial ice will impact above the limit at which the semi-submersible shall be strengthened against a ship impact. The relative elevation between the two objects is ±9.6 m and ±11 m for 50 % and 90 % probability of non-exceedance which is 8 m above the waterline and 3 m above the area which should be strengthened against a ship impact. Sea state 3 is associated with long wave periods and high waves and all shapes and masses in this sea state lead to an impact both above and below the extent of the area strengthened against ship impact. For sea state 1 and 2 the vertical impact is below the area which should be strengthened against a ship impact.

Table 7: The vertical impact elevation for an impact between glacial ice and a semi-submersible.

Shape	Length (L)	Mass	Ref.elev.	Sea state 1		Sea state 2		Sea state 3	
				median	90 %	median	90 %	median	90 %
	[m]	[tons]	[m]	[m]	[m]	[m]	[m]	[m]	[m]
Spheroid	12	390	-2.3	±7.2	±8.0	±6.5	±7.3	±9.6	±10.8
	15	765	-2.9	±4.2	±4.7	±6.7	±7.5	±9.6	±10.8
Cuboid	12	744	-3.2	±5.7	±6.3	±5.4	±6.0	±8.9	±10.0
	15	1432	-3.9	±3.8	±4.3	±5.7	±6.3	±9.0	±10.2

Table 8: The vertical impact elevation and horizontal velocity (sway) between the large cuboid and the semi-submersible for different return periods of the sea states.

Shape	Return period of sea state	Hs	Tp	Gamma γ	Vertical elevation		Horizontal velocity	
					Median	90 %	Median	90 %
	[year]	[m]	[s]	[-]	[m]	[m]	[m/s]	[m/s]
Cuboid	1	4.9	6.5	5.0	±3.1	±3.5	±2.6	±2.9
	1	8.6	12.0	2.9	±4.3	±4.8	±3.5	±4.0
	1	9.8	14.8	1.4	±5.1	±5.7	±3.4	±3.8
	10	5.5	6.5	5.0	±3.5	±3.9	±2.9	±3.3
	10	10.3	13.0	3.0	±4.9	±5.5	±3.9	±4.4
	10	11.8	16.4	1.3	±6.9	±7.7	±3.7	±4.1
	100	6	6.5	5.0	±3.8	±4.3	±3.2	±3.6
	100	12	14	3.0	±5.7	±6.3	±4.2	±4.7
	100	13.8	18	1.2	±9.0	±10.2	±3.9	±4.4

Notes. γ is the peak enhancement factor in the JONSWAP spectrum.
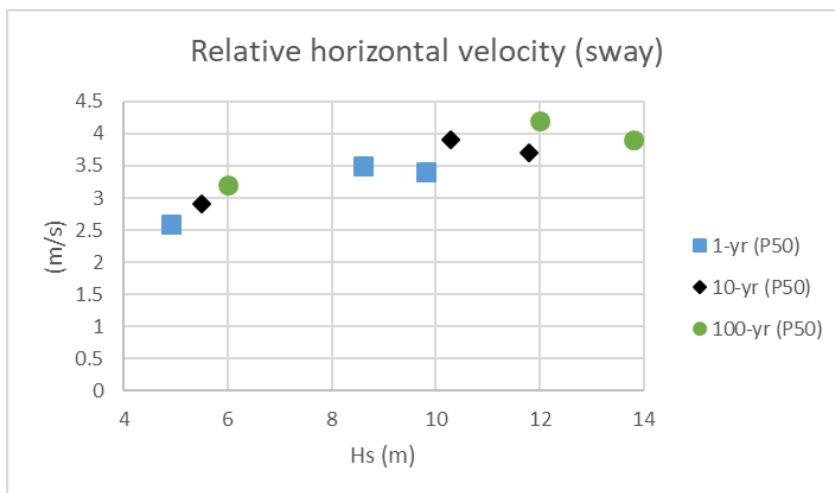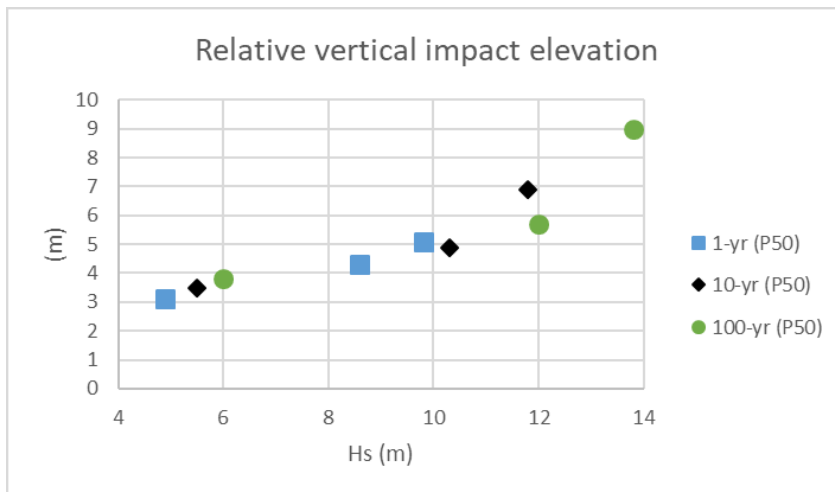
Figure 24: Relative impact elevation (upper) and horizontal relative sway velocity (lower) between the large cuboid and the semi-submersible.

The significant response per Hs for the relative vertical displacement between the large cuboid and the semi-submersible is shown in Figure 25. The significant response is defined as the mean of the one-third largest responses in the response spectrum, and the curve is a result of combining the RAOs for the relative motion with JONSWAP wave spectra with unit Hs and a constant peak shape factor ($\gamma = 3.0$). For small values the curve shows that the relative displacement between the glacial ice and the semi-submersible is small and the peaks indicate for which peak periods (Tp) the largest relative motions will occur assuming unit Hs. The sea states analysed (Table 4) are also included in the figure, and the two-peaked shape of the curve is a result of the two-peaked RAO for the relative vertical motion, refer to Figure 12. From the figure, it is clear that a sea state with a peak period of 8.5 s will give large relative motions between the glacial ice and the semi-submersible. Scatter diagrams for Hs and Tp are included in the metocean design basis [19] and it is seen that sea states with Tp between 8 and 9 s correspond to 14 % of all sea states per year. Similarly, the sea state considered in this analysis with Tp equal to 6.5 s corresponds to 13 % of all sea states per year while 71 % of all sea states per year have Tp less than 10 s. Hence, sea states with Tp in the range 8 to 10 s are good candidates for further analysis.

Since the different glacial ice shapes have similar motion RAOs it is expected that the results for the different sizes and shapes will have a similar trend as presented in Figure 25 for the large cuboid. The main difference is most likely the position and amplitude of the peak around Tp=8.5 s since this peak is related to the motion of the glacial ice.

Figure 26 shows the significant response per Hs for the relative horizontal velocity (sway) between glacial ice and the semi-submersible. The wave direction is 270°. A linear, decaying trend is observed for peak periods larger than 6 s.
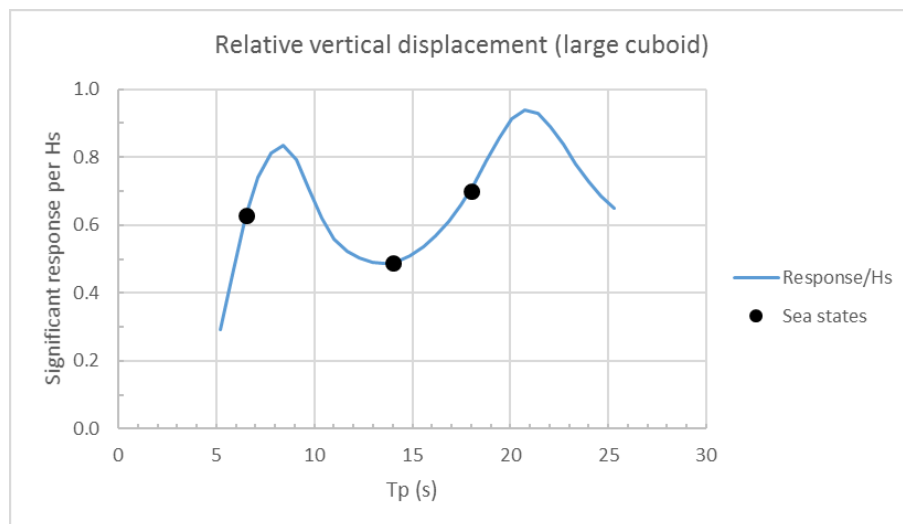
Figure 25: Significant response per Hs for the relative vertical displacement between glacial ice (large cuboid) and semi-submersible.
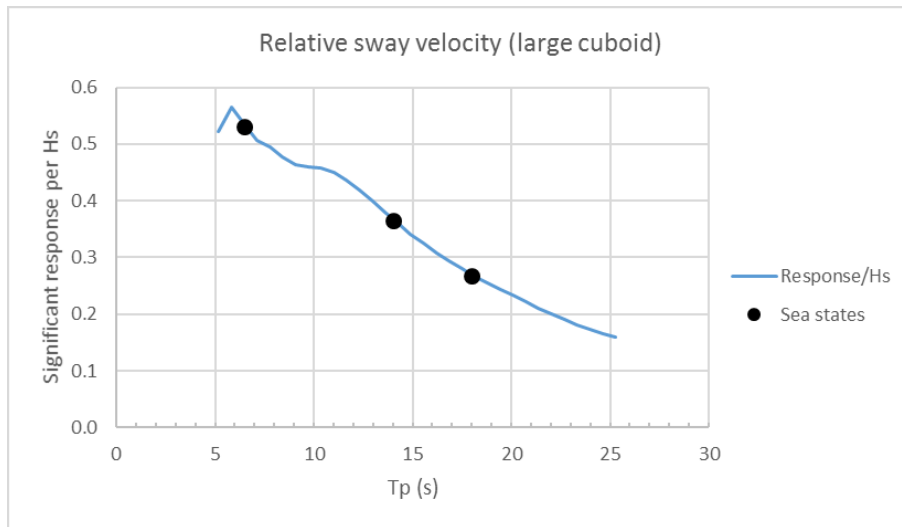
Figure 26: Significant response per Hs for the relative horizontal velocity (sway) between glacial ice (large cuboid) and semi-submersible.

5.2 Other structural elements

The main assessment in this report investigate the possibility that glacial ice of a simplified shape and a certain size may hit within the zone which is required to withstand a ship impact. However, glacial ice shapes and sizes naturally vary. Unlike ships, that can be assumed to only hit on the outer circumference of the legs of the semi-submersible (Figure 2), glacial ice may hit structural components between the legs and under the semi-submersible. This is possible given that the glacial ice is small enough to enter in-between the legs of the semi-submersible. In this area, sensitive equipment like drill string, riser etc. is located, equipment which normally is not strengthened to withstand a ship impact when it is protected by the legs of the semi-submersible.

5.3 Impact energy

The energy available as deformation energy in an impact between a facility and a piece of glacial ice may be quantified in two steps. First step is to find the kinetic energy of a free-floating piece of glacial ice via

$$E_i = \frac{1}{2}(m_i + a_i)v_i^2 \tag{8}$$

Here, v_i is the velocity of the glacial ice, m_i is the body mass and a_i is the added mass. The velocity and mass components in the sway mode of the motion are used which gives the horizontal motion of glacial ice towards the semi-submersible. Because the semi-submersible is a floating facility it affects the relative velocity at impact. This can be accounted for by adjusting the available energy for deformation from a free-floating body after DNVGL-RP-C204 [24]:

$$E_{impact} = E_i \cdot \frac{\left(1 - \frac{v_s}{v_i}\right)^2}{1 + \frac{m_i + a_i}{m_s + a_s}} \tag{9}$$

where v_s, m_s, a_s are the velocity, body and added mass of the semi-submersible (facility). For the semi-submersible used in the present study (25 000 tonnes) the impact energy is reduced by 2-6 % compared to the kinetic energy of the free-floating piece of glacial ice (assuming $v_s = 0$). The impact

energies quoted from regulations, rules and standards (Section 3) can be considered as kinetic energy of free floating ships. To estimate comparable kinetic energies the adjustment of kinetic energy in the presence of a facility is not included in the results presented below.

The kinetic energy for the glacial ice is estimated per sea state and presented in Table 9. The kinetic energy associated with the median velocity varies between 7 and 23 MJ for the shapes, masses and sea states considered. For Case 2 the estimated kinetic energy is lower than 14 MJ which suggests that, compared with the kinetic energy considered in a ship impact, the glacial ice will not be a challenge (if the impact is within the area that should be strengthened against ship impact). For cases 3, 5 and 6 the kinetic energy exceeds 14 MJ in some sea states which is the limit used for ship impact in the NMA regulations.

Table 9: Estimated kinetic of glacial ice energy for the shapes, masses and sea states considered.

Glacial ice	Sea state	Velocity [m/s] Median	90 %	Mass [tons] Body	Added	Kinetic energy [MJ] Median	90 %
Case 2	1	4.7	5.2	390	274	7	9
	2	4.7	5.3	390	212	7	8
	3	4.3	4.8	390	206	6	7
Case 3	1	4.4	4.9	765	573	13	16
	2	4.7	5.2	765	416	13	16
	3	4.3	4.8	765	404	11	13
Case 5	1	3.7	4.1	744	774	10	13
	2	4.3	4.8	744	588	12	15
	3	4.0	4.4	744	575	11	13
Case 6	1	3.2	3.6	1432	1379	14	18
	2	4.2	4.7	1432	1153	23	29
	3	3.9	4.4	1432	1128	19	25
10 year, 1	Hs=5.5 Tp=6.5	2.9	3.3	1432	1379	12	15
10 year, 2	Hs=10.3 Tp=13	3.9	4.4	1432	1153	20	25
10 year, 3	Hs=11.8 Tp=16.4	3.7	4.1	1432	1128	18	22
1 year, 1	Hs=4.9 Tp=6.5	2.6	2.9	1432	1379	10	12
1 year, 2	Hs=8.6 Tp=12	3.5	4.0	1432	1183	16	21
1 year, 3	Hs=9.8 Tp=14.8	3.4	3.8	1432	1153	15	19

Notes
- The sway mode of added mass is reported (A_{22}) and is taken at the zero up-crossing period (Tz) for each sea state.
- For case 6, analyses combining 1 and 10-year sea states are also included in the table.

6 COMPARISON WITH SHIP IMPACT

6.1 General

The study does not consider the probability of the joint event of an interaction with glacial ice in a sea state with a given return period. Instead, it is assumed that the glacial ice will interact with the facility in selected sea states with annual probability of exceedance of 10^{-2}. The joint probability of these two events are significantly lower than 10^{-2} and perhaps even lower than 10^{-4} for many locations in the Barents Sea.

NORSOK N-003 (2017) suggests that an iceberg impact should be combined with a 10-year sea state in ULS and a 1 year sea state in ALS. The current study analysed an iceberg impact using 3 sea states from the Hs-Tp curve corresponding to a 100-year sea state. From the scatter plot in [19] the wave height corresponding to a wave period of 14 s (same as sea state 2) with a 10-year return period is 11 m. This is 10 % lower than the wave height in sea state 2. The reduction in significant wave height transfers directly to the resulting relative vertical displacement (Figure 25) and shows that sea states with a 10-year return period give nearly similar results as 100-year return period. The same 10 % reduction in wave height is found for sea state 1. For sea state 3 there is no corresponding 10-year wave height because this is a peak Hs value on the Hs-Tp contour.

6.2 Area of impact

Drifting glacial ice follows to a certain extent the particle track of the waves. This suggests that there will be a high forward velocity component at the crest of the wave and a backward velocity component at the trough (forward is assumed towards the facility). This could indicate that the "high impacts (upper part of the column)" may be more relevant to investigate further compared to the lower impacts. However, as glacial ice has a very low draft and since the reference point often is quite far below the waterline it cannot be concluded whether a high or a low impact is more likely. The shape of glacial ice also varies significantly and the shapes in the present study are without any extremities. Such extremities may result in impact on a facility both above and below to the vertical location of the centre of gravity which is used as a reference point in the present study. The results for Case 6 (Table 7) could serve as an example. Table 10 shows the results when the reference elevations correspond to the top and bottom corner (Figure 23) and only the positive elevation (top corner) and the negative elevations (lower corner) are included. The extremities will, in all sea states, impact either above or below the area which shall be strengthened against a ship impact.

Table 10: The vertical impact elevation for an impact between glacial ice and a semi-submersible using the elevation of the cuboids corners as reference elevation.

Shape	Length (L)	Mass	Ref.elev.	Sea state 1		Sea state 2		Sea state 3	
				median	90 %	median	90 %	median	90 %
	[m]	[tons]	[m]	[m]	[m]	[m]	[m]	[m]	[m]
Cuboid (top.pt)	12	744	1	6.7	7.3	6.4	7.0	9.9	11.0
Cuboid (bt.pt)	12	744	-7.3	-13	-13.6	-12.7	-13.3	-16.2	-17.5

During transit the draught of the semi-submersible is "transit-draft" which in practice means that parts of the pontoons are exposed to ship impact. The NMA regulations requires that ship impact is considered in transit mode. This means that parts of the area around the pontoons shall be able to withstand an impact (illustrated in Figure 2). This may be considered an advantage considering that the glacial ice analysed in the present study may hit most parts of the semi-submersible below the waterline including different parts of the pontoons. Other structural elements not required to withstand a ship impact is discussed in section 5.2.

6.3 Impact energy

The requirement to withstand a ship impact is 14 MJ for floating mobile offshore units (Section 3). This value is based on a ship, 5000 tons, drifting at 2 m/s with an added mass of 40 % and a sideways collision. The drift speed of 2 m/s is based on an operational limit that no ship can approach the facility for wave heights above 4 m [25]. This assumes that the drift speed of a free-floating ship relates to the significant wave height by:

$$v_{ship} = 0.5 Hs \tag{10}$$

In the present analysis, the estimated velocity is the extreme values for a 3-hour period. Because the supply ships are longer and heavier than the analysed glacial ice it is expected that the response of the facility for a sea state are of smaller magnitude compared to the glacial ice analysed in the present study. The study did find that the kinetic energy for free-floating glacial ice with waterline 12-15 m have similar or greater kinetic energy than 14 MJ which is used as basis for ship impact. If kinetic energy alone indicates the facilities capability to withstand an impact with glacial ice this shows that facilities cannot withstand an impact with glacial ice of this size and shape in the analysed sea-states. However, the impact characteristics are different in a ship impact compared to an impact with glacial ice and section 7 investigates this in greater detail.

7 GLACIAL ICE DESIGN LOADS

7.1 General

For the purpose of determining ice design loads under design conditions involving ice impact against an offshore structure, ISO 19906 recommends the use of pressure-area formulations. These may be used to predict, under the event of ice-structure impact, a spatially averaged ice crushing pressure over a specified nominal contact area. ISO 19906 specifies one particular pressure-area formulation for this purpose, and this formulation is intended to be used for any type of ice impact, irrespective of the type of ice (e.g. glacial ice or multiyear sea ice), namely:

$$p = C_p A_N^{D_p} \tag{11}$$

where A_N is the nominal contact area and C_p (multiplier) and D_p (exponent) are coefficients determined from a set of ship rams data.

ISO 19906 also recommends the pressure-area formulation specified therein for the purpose of determining, by probabilistic analysis, an ice design load associated with a prescribed annual exceedance probability. In this case, the formulation involves C_p and D_p as 'random coefficients' (ISO 19906), the purpose of which is to take into account the apparent random nature of the fracture processes in the ice during impact. The required characteristics of these 'random coefficients' are fully described in ISO 19906. The relevant sections therein are:

> A.8.2.4.7.3 'Impact actions', and

> A.8.2.4.3.5 'Global ice pressures from ship ramming tests'.

Both sections appear under section A.8.2.4 'Global ice actions', under A.8.2 'Ice actions', under A.8 'Actions and action effects'.

In particular, ISO 19906 section A.8.2.4.7.3 states that:

> 'For probabilistic solutions, the contributing parameters can be random, and the contact areas or widths should reflect the distributions of measured ice feature shapes and ice impact orientations with respect to the structure. The distribution of pressures should reflect the average impact pressure over each interaction. For impact situations, random values of the pressure coefficients, C_P and D_P, can be used; see Equation (A.8-24).'

Here, a reference is made to the pressure-area equation with 'random coefficients' specified in ISO 19906 section A.8.2.4.3.5. According to ISO 19906, the coefficients in this equation 'have been calibrated using a large database of ship rams with multi-year ice'.

The characteristics of the pressure-area formulation given in ISO 19906 may be illustrated as shown in Figure 27 below: the black dash-dot curve is the median curve, were, for a given contact area, the formulation predicts that it is as likely to observe a spatially averaged ice crushing pressure above that curve as below it; the blue continuous curve shows, for a given contact area, the most probable spatially averaged ice crushing pressure over that contact area. The black dotted curves represent the anticipated dispersion in a number of realizations of the ice crushing pressure at a given contact area: in this case they can be considered to collectively represent a 90 % prediction interval for the spatially averaged crushing pressure over a given contact area. This figure illustrates the highly uncertain nature of ice crushing pressures as predicted by the ISO 19906 pressure-area formulation.

The ISO 19906 pressure-area formulation is based on linear regression of data in the log-log diagram, and the resulting pressure distribution is essentially log-normal. The formulation involves a highly area-

dependent dispersion about the median line (which is the mean line in the log-log diagram). Because of this behaviour, the curve representing the 'most probable' pressure deviates considerably from the median line whenever the nominal contact area is very much different from 1 m². This behaviour is a direct result of the particular way in which randomness has been incorporated into the pressure-area formulation.
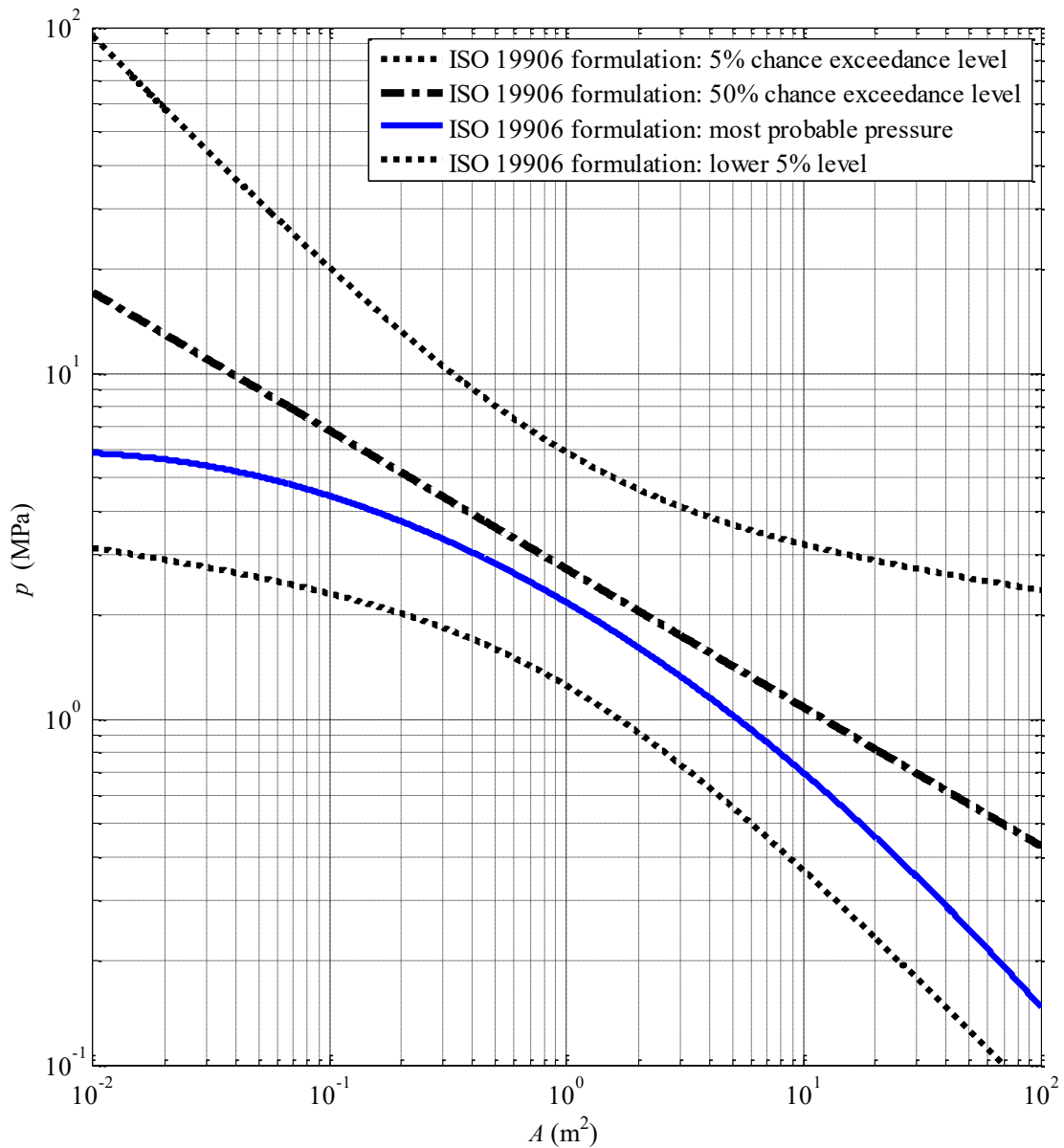
Figure 27: The essential characteristics of the probabilistic pressure-area formulation given in ISO 19906.

ISO 19906 recommends to use the value of -0.7 for the exponent D_p in the local pressure estimations, while value of -0.4 is given for the estimation of the average global pressure estimations.

The values for the multiplier C_p varies depending on the background data, return period to be considered and the assumed annual exposure to the ice impact. Some of the values for C_p referenced in ISO-19906 and considered for its update are 7.4, 9.6, 16.37 and 22.13.

7.2 A pressure-area model for glacial ice impact

Based on the pressure-area formulation from ISO 19906 a deterministic pressure-area model is made. The model assumes that all deformation takes place in the glacial ice and gives contact pressure as function of increasing ice deformation and contact area. The model assumes that the impacted structure is infinitely strong. The results can be compared with capacity results from non-linear analyses of the structure to evaluate the response to the ice load.

The geometry of the glacial ice shape is represented by a set of contours, where each contour is contained in a horizontal plane and represents the horizontal extent of the iceberg at a specified elevation. During the interaction simulation, the glacial ice moves along a linear trajectory at constant steps, referred to as penetration steps and the contact area is estimated. In this study, the impact energies established from the Wadam analysis are used as input. At each penetration step the following quantities are calculated:

- nominal contact area;

- crushing pressure, if the area-dependent model is applied. Otherwise, the crushing pressure is assumed to be constant;

- penetration force and overturning moment applied to the structure;

- loss in kinetic energy due to the total penetration force.

The penetration steps are continued as long as the kinetic energy of the glacial ice is non-zero.

In order to compare with results from Non-linear Finite Element analyses (Case 1, Case 2 and Case 3 in Chapter 8), the pressure-area model is used to simulate the interaction between glacial ice and a rigid facility. For all three cases two different crushing models are applied. The crushing model is either a constant crushing pressure of 1.5 MPa (proposed by ISO 19906 for local design areas >10 m²) or following the power law (11) with $C_p = 7.4$ and $D_p = -0.7$. Figure 28 shows the results and the dependencies between contact area, impact force, deformation energy and penetration depth (of the glacial ice) as well as contact area/crushing pressure curve. The penetration/deformation step is 0.05 m.
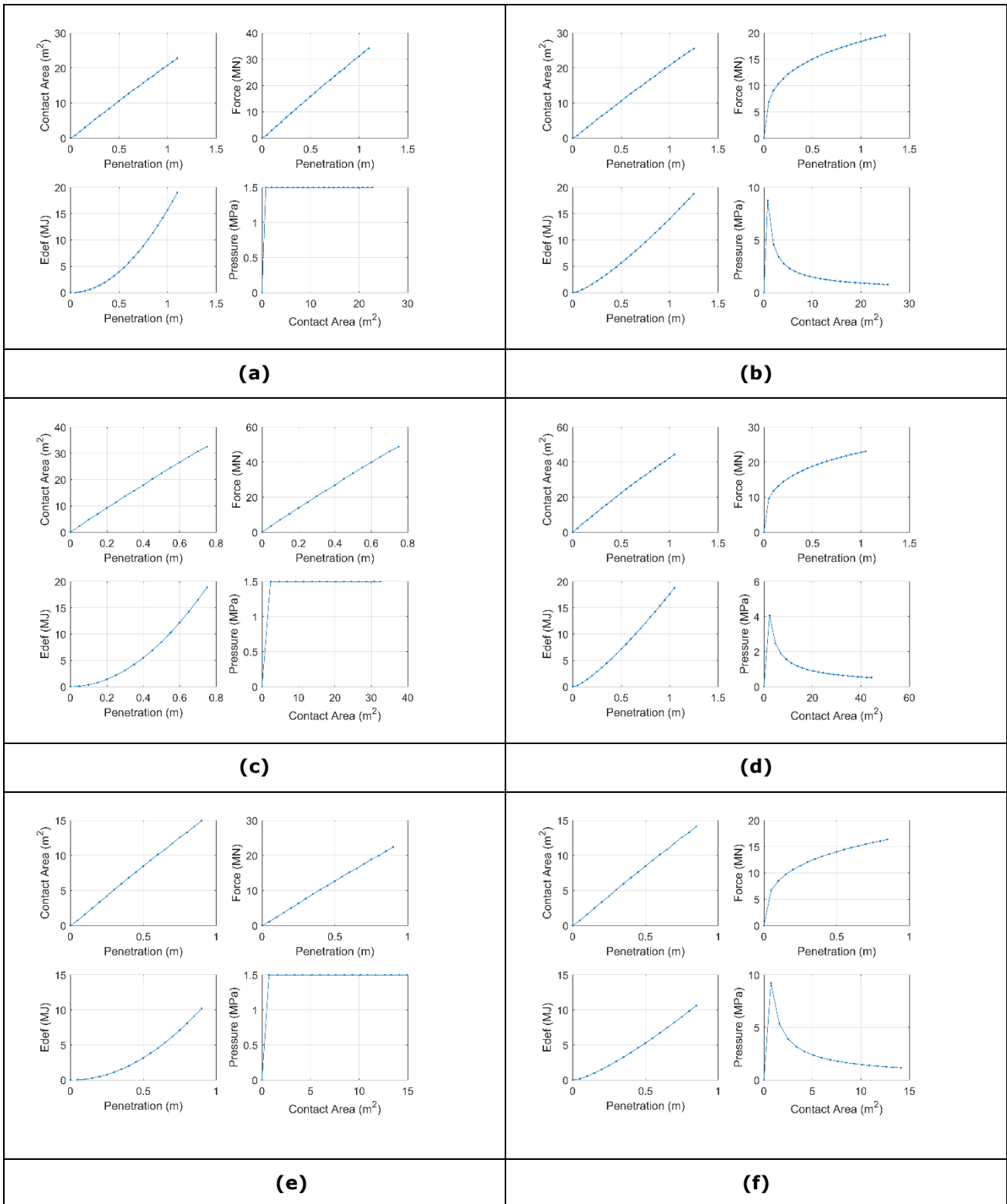
Figure 28: Results of the pressure-area model. Constant pressure (1.5 MPa) on the right side and crushing pressure from Eq. (11) on the left side. Case 3 – (a), (b), Case 3 rotated 90 degrees with respect to the column and Case 2 – (e), (f).

8 IMPACT ANALYSIS USING NON-LINEAR FE ANALYSIS

8.1 General

To assess structural capacity of a stiffened plate in a semi-submersible for glacial ice impact, the framework for simplified analyses for ship collision in DNVGL-RP-C204 [24] was applied.

A "typical" drilling rig design was selected for modelling and analyses with input from DNV GL Offshore class (Section 8.2). Based on information from Chapter 5 and information on the extent of ship impact protected areas, a section of a typical drilling rig column was modelled. The modelling and FE analyses follow the guidelines in DNVGL-RP-C208 [26]. The selected impact location is in an area designed for ship impact loads.

The energy absorption in the drilling rig (facility) and the glacial ice were evaluated separately under the assumption that one of the objects is stronger than the other. The glacial ice was initially considered as a rigid body in the FE analyses and is documented in section 8.3.3. One analysis with the glacial ice modelled as uniform pressure was also included (section 8.3.4). In parallel, a simplified analysis based on the assumption that the facility is a perfect rigid body and the impact energy dissipates entirely due to crushing of the ice was conducted (section 7).

The method applied is best suited for what is referred to in DNVGL-RP-C204 [24] as *strength design*, i.e. ensuring that the '*the installation is strong enough to resist the collision force with minor deformation*'. The FE analyses with rigid glacial ice objects can however also be considered for *ductile design,* i.e. requiring that the facility can absorb all the impact energy. The approach applied is similar to the common simplified design approach for design against accidental ship impact loads (i.e. assessing response of ship and platform independently).

For ship impact design, more advanced methods are becoming increasingly popular for high energy impacts. These methods model the collision with two deformable bodies using explicit FE software. Such analyses are very demanding with respect to computational resources and have become more available to the engineering community in the last few decades. Guidelines for such analyses is included in the latest revision of DNVGL-RP-C208 [26]. For ice impacts this approach has been tested by the research community using material and failure models for the ice, see for example [27], [28] and [29]. For ice the main challenge with this approach is the lack of experimental data to establish a fundamental material model. In the lack of a fundamental material model the simulations are calibrated against area penetration models or single impact tests [28] and the calibrated material models are thus not reliable for general use. Advanced methods are therefore not considered suitable for design until more knowledge is gained.

8.2 Selection of typical column

Drawings for three different rig designs were studied based on discussions with DNV GL Offshore class. The selected rig designs are considered relevant for operations in the Barents Sea.

Table 11 to Table 13 show a comparison of the main dimensions and the structural components in the pontoons and the columns for the three facilities. As seen, the dimensions are similar for all facilities. The column of the DESIGN 2 design is the one with the smallest dimensions, and the waterline geometry of a column in this facility was selected for modelling.

The selected area for modelling is shown in Figure 29 to Figure 31. It is pointed out that the impact energy is based on a hydrodynamic analysis with circular columns while the impact analysis assumes

columns with a rectangular cross section with rounded corners. This difference is believed to be of minor importance for the impact analysis since the glacial ice vary both in shape and size.

**Table 11: Main dimensions of rig designs considered for the study.**

Design, overall	DESIGN 1	DESIGN 2	DESIGN 3
Length [m]	122.6	106.75	116
Breadth [m]	79	73.7	76.7
Operating Draught [m]	23.5	21	23.15
Air Gap (operating) [m]	13	13	12.6
Survival Draught [m]	21.5	19	19.15
Air Gap (survival) [m]	15	15	16.6

Table 12: Pontoon dimensions of rig designs considered for the study.

Pontoon	DESIGN 1	DESIGN 2	DESIGN 3
Length [m]	122.6	106.75	110.5
Breadth [m]	17.8	16.2	16.25
Depth [m]	11.4	10.4	9.75
Frame distance [mm]	1920	2250	2600
Frame web height [mm]	1500	1400	1625
Frame web thick [mm]	22	18	15
Frame flange width [mm]	300	300	250
Frame flange thick [mm]	20	25	25
stiffener distance [mm]	640	650	650
Stiffener type	L300x90x11x16	HP 300x11	HP 340x12
Shell plating [mm]	16	16	14

**Table 13: Column dimensions of rig designs considered for the study.**

Column	DESIGN 1	DESIGN 2	DESIGN 3
Number of	6	4	4
Length (max) [m]	13.4	15.2	17.55
Breadth [m]	17.8	16.2	16.25
Stringer distance min [mm]	1720	2350	2500
Stringer distance max [mm]	2560	3100	3000
Stringer web height [mm]	1000	900	1000
Stringer web thickness [mm]	18	16	20
Stringer flange width [mm]	200	200	300
Stringer flange thick [mm]	20	20	30
Stiffener distance [mm]	640	630	650
Stiffener type	L300x90x11x16	HP 240x12	HP 280x12
Shell plating [mm]	14	14	15
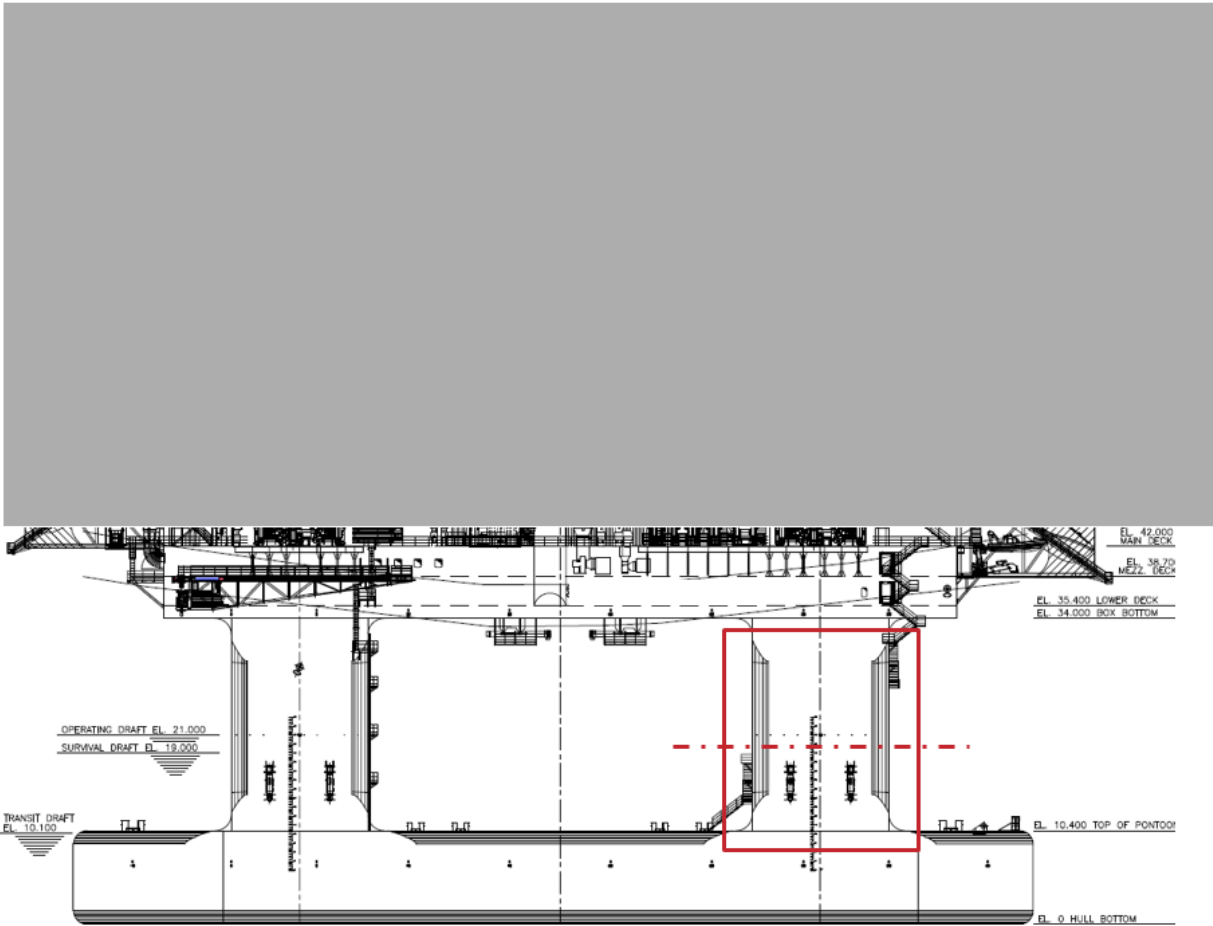
Figure 29: Column of DESIGN 2 selected for FE modelling.
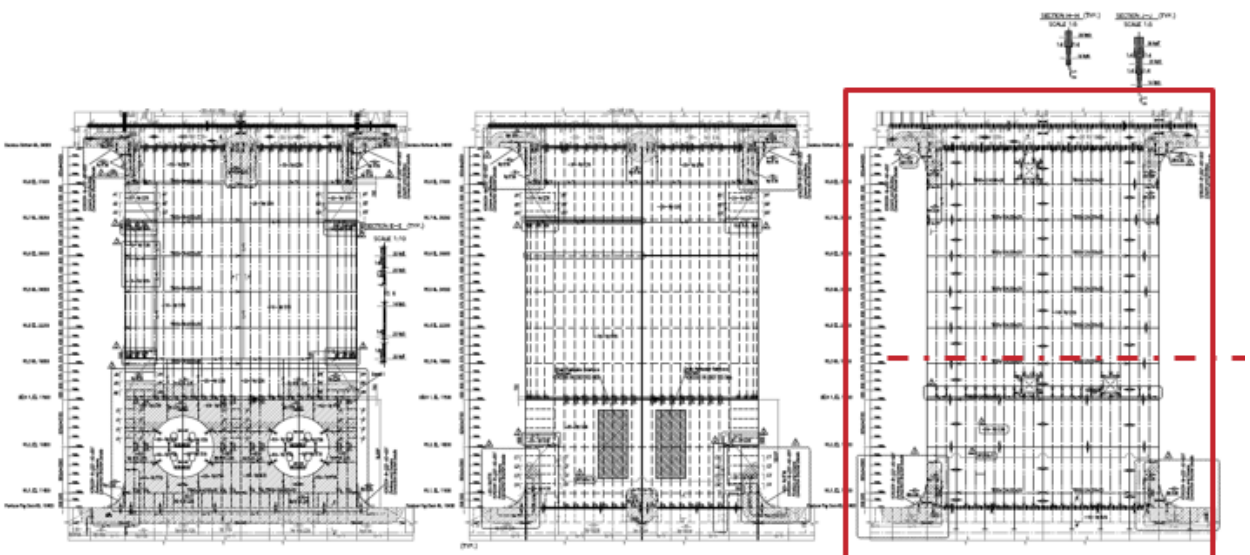
Figure 30: Column of DESIGN 2 selected for FE modelling, selected elevation.
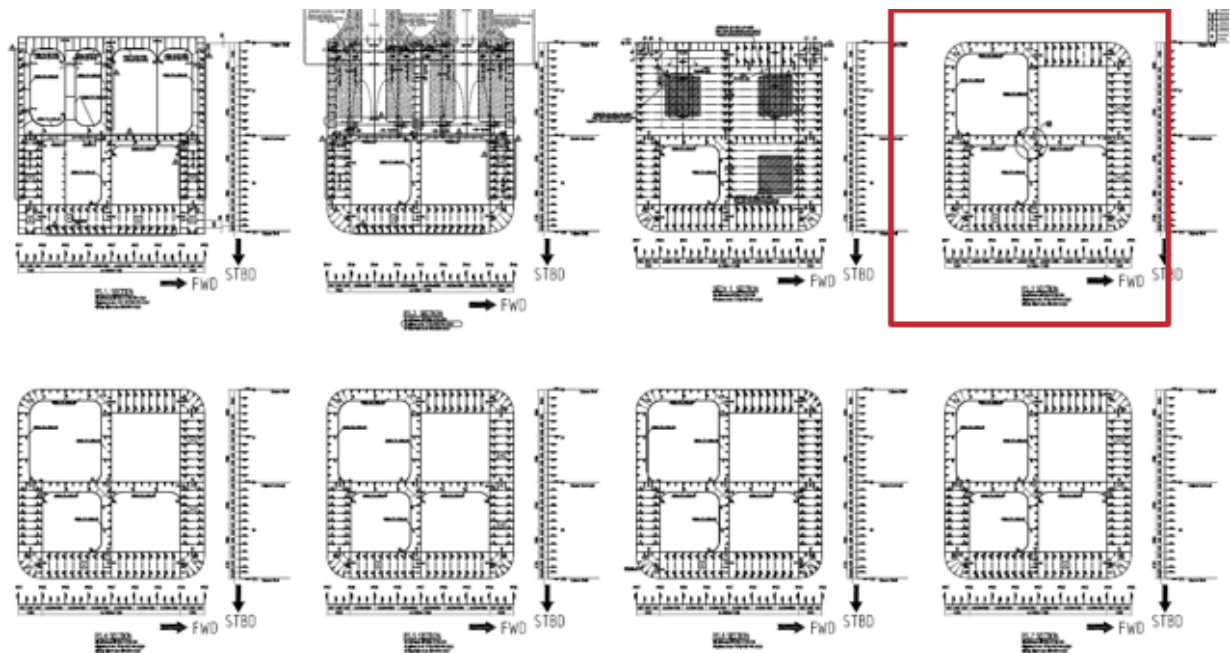
Figure 31: Column of DESIGN 2 selected for FE modelling, selected ring section.

8.3 Non-linear FE Analyses

8.3.1 General

The modelling and analyses were performed using Abaqus [30]:

- Abaqus/CAE-2017 for modelling and post processing

- Abaqus/Explicit for analyses

8.3.2 FE model

A section of the DESIGN 2 column was modelled in detail using ring section 3 section shown in Figure 30 and Figure 31. This model part, shown in Figure 32, was copied to build up a longer segment of the column. The assembled model of the column is shown in Figure 33. The model is fixed in all directions at the lower elevation, and fixed in horizontal directions at the upper elevation. The model was meshed with element type S4R which is the default 4-node non-linear shell element with reduced integration scheme. A mesh corresponding to roughly 5tx5t (75 mm) was selected for the impact area, where t is the thickness of the outer shell. Outside this area, a coarse mesh (200 mm) was used to save simulation time. The mesh is shown in Figure 34. The column material has a yield strength of 355 MPa. The material curve used in the FE model is a characteristic curve according to DNVGL-RP-C208 [26] and is shown in Figure 35. A fracture criteria based on 1st principal strain was used. The limiting strain value was calculated to 7 % according to DNVGL-RP-C208 based on mesh size, plate thickness and material quality. As Abaqus can only use equivalent strain as fracture criteria, a triaxiality dependent equivalent strain limit was used, see Figure 36.

The relationship between the equivalent strain and the 1st principal strain as function of triaxiality was derived in the following way:

- Define a range of 2-d stress states that give the triaxiality range. ($\sigma_1=1$, $\sigma_2<=1$ $\sigma_3=0$)
- For each stress state
  - Calculate the hydrostatic stress $\sigma_h = \frac{1}{3}(\sigma_1 + \sigma_2 + \sigma_3)$
  - Calculate the equivalent stress $\sigma_{eq} = \sqrt{\frac{1}{2}(\sigma_1 - \sigma_2)^2 + (\sigma_2 - \sigma_3)^2 + (\sigma_3 - \sigma_1)^2}$
  - Calculate the triaxiality $T = {\sigma_{eq}}/{\sigma_h}$
  - Use the Levy-Mises flow rule to calculate the incremental strains
  - Assuming constant stress state and constant 1st principal strain, calculate corresponding strain components and equivalent strain.
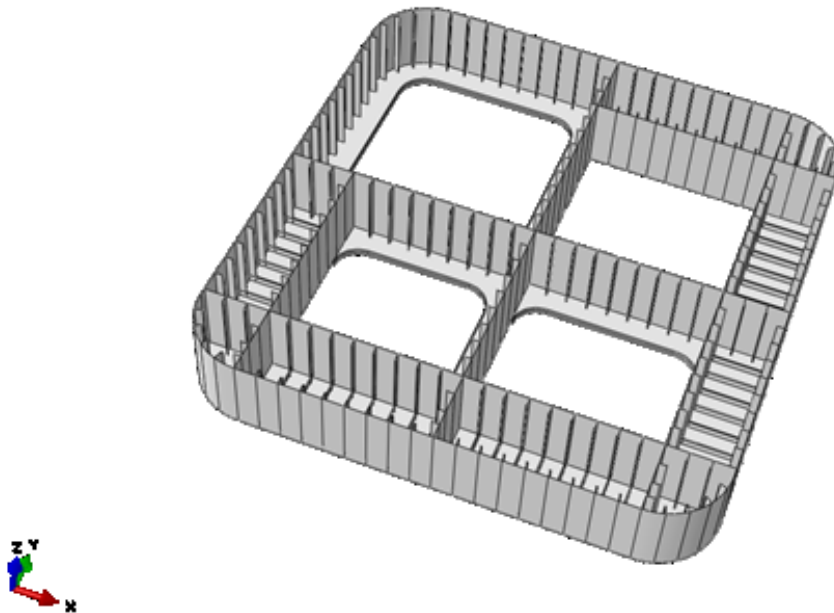

**Figure 32: FE model of ring section 3 section.**
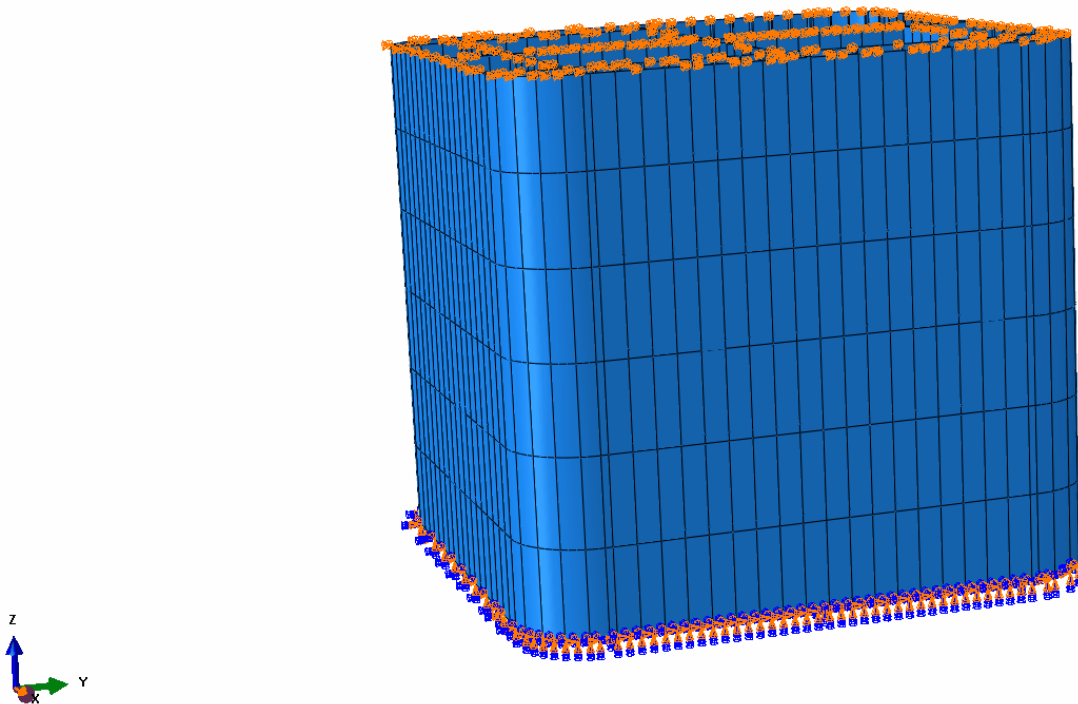
Figure 33: Column model, six ring sections (copies of ring section 3).
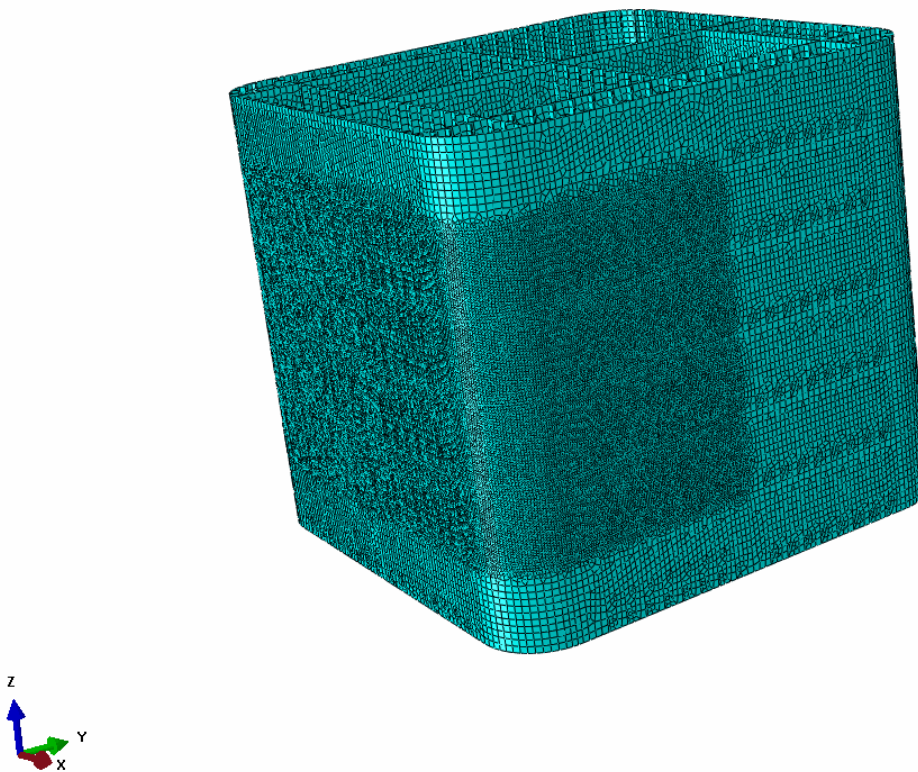
Figure 34: FE Mesh, 75 mm(5tx5t).
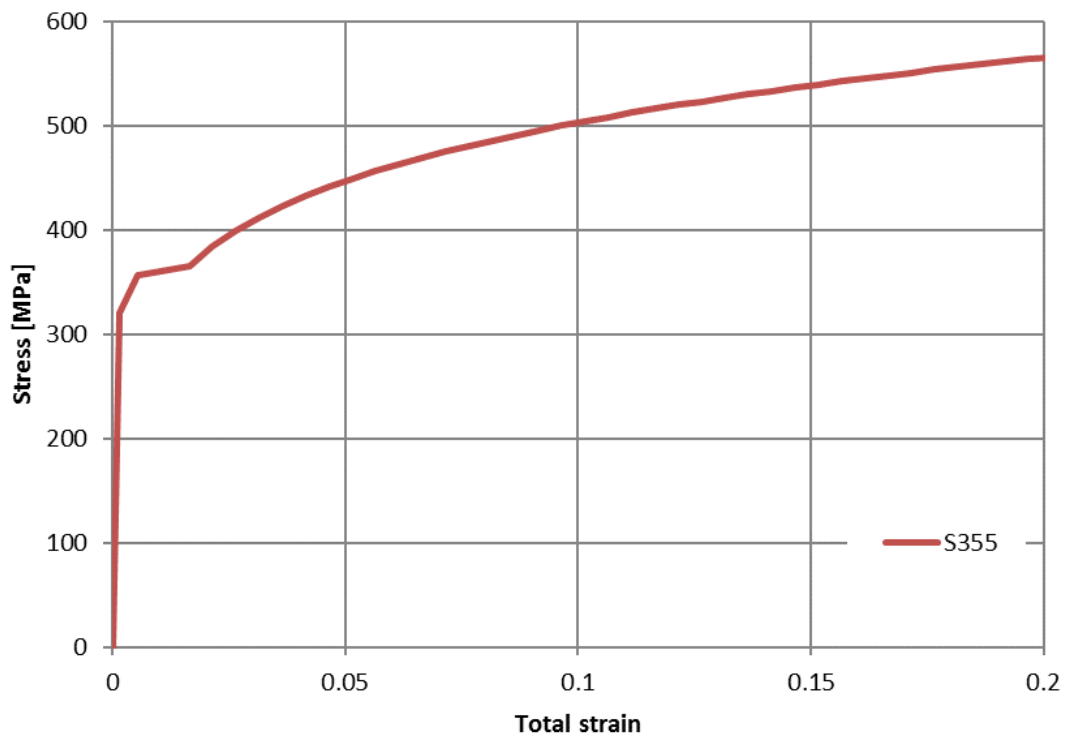
Figure 35: Material curve, characteristic strength, S355.
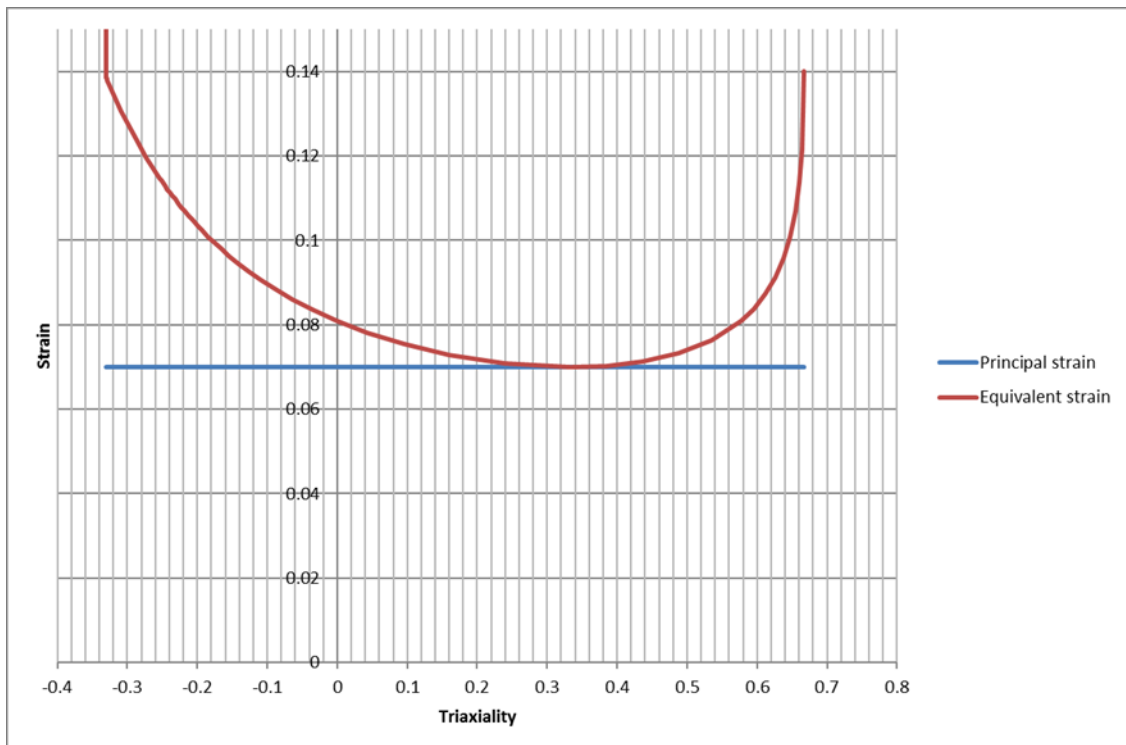
Figure 36: Equivalent strain fracture criteria as function of triaxiality ratio, given constant 1st principal strain.

8.3.3 Analyses, rigid Ice objects

8.3.3.1 Analysed cases

Five analyses with rigid objects were performed to investigate how the contact force and energy absorption in the steel structure as function of deformation varies with the shape of the impacting object.

The spherical Ice objects given in Table 14 were used. For the largest object (15x10.4) two analyses were performed, one with the narrow end hitting the structure (Case 1) and one with the wide end hitting the structure (Case 2). For the three smaller objects the analyses were performed with the narrow end hitting the structure first, minimizing the contact area.

Table 14: Considered Ice objects.

Case	Ice object	2c(m)	2a(m)	Mass(t)
Case 1	Spheroid 15x10.4	15	10.4	765
Case 2	Spheroid 15x10.4W	15	10.4	765
Case 3	Spheroid 12x8.3	12	8.3	390
Case 4	Spheroid 10x7	10	7	230
Case 5	Spheroid 7x5	7	5	79

8.3.3.2 Analysis setup

In all cases the Ice object is pushed with a constant velocity of 3 m/s into the column structure. The Ice object is fixed in all other degrees of freedom. Contact surfaces were defined on the Ice object and the column. Self-contact was also defined for the inner structure of the column. The Ice object was positioned to impact between horizontal and vertical frames as shown in Figure 37.
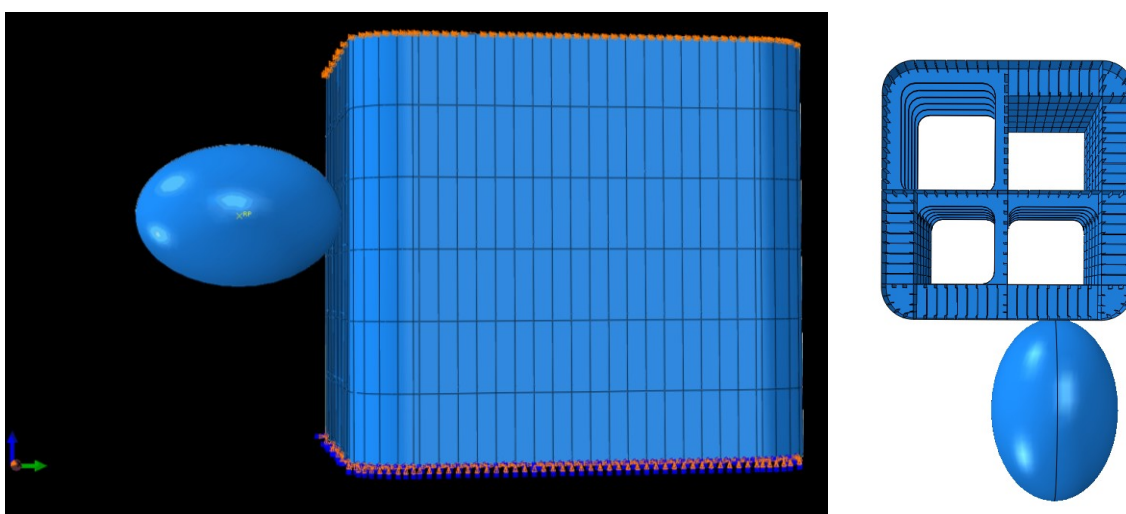
**Figure 37: Analysis setup.**

8.3.3.3 Results

The main results for the analyses are shown in Figure 38 to Figure 41. The contact force, deformation energy, contact area and average contact pressure are presented as function of Ice object indentation. The deformation when outer shell fractures is 270 to 330 mm for all simulations except for case 2 where the outer shell fractured at 420 mm.

The curves are stopped when fracture of the inner shell occur. The smaller objects penetrate more locally, while larger objects give global deformations in addition. This leads to the results that smaller (more pointed) objects quicker penetrate the inner shell. The fracture of the inner shell designates the

situation where moderate (few compartment) damage occurs and where larger volume internal water filling is expected.

Figure 42 shows the development in contact area and contact pressure. As seen, the pressure is not uniform within the contact area, the maximum pressures at hard points (e.g. stiffeners) are in the order of 50 MPa. Note that also the mesh discretisation to some extent influence on the stress distribution.
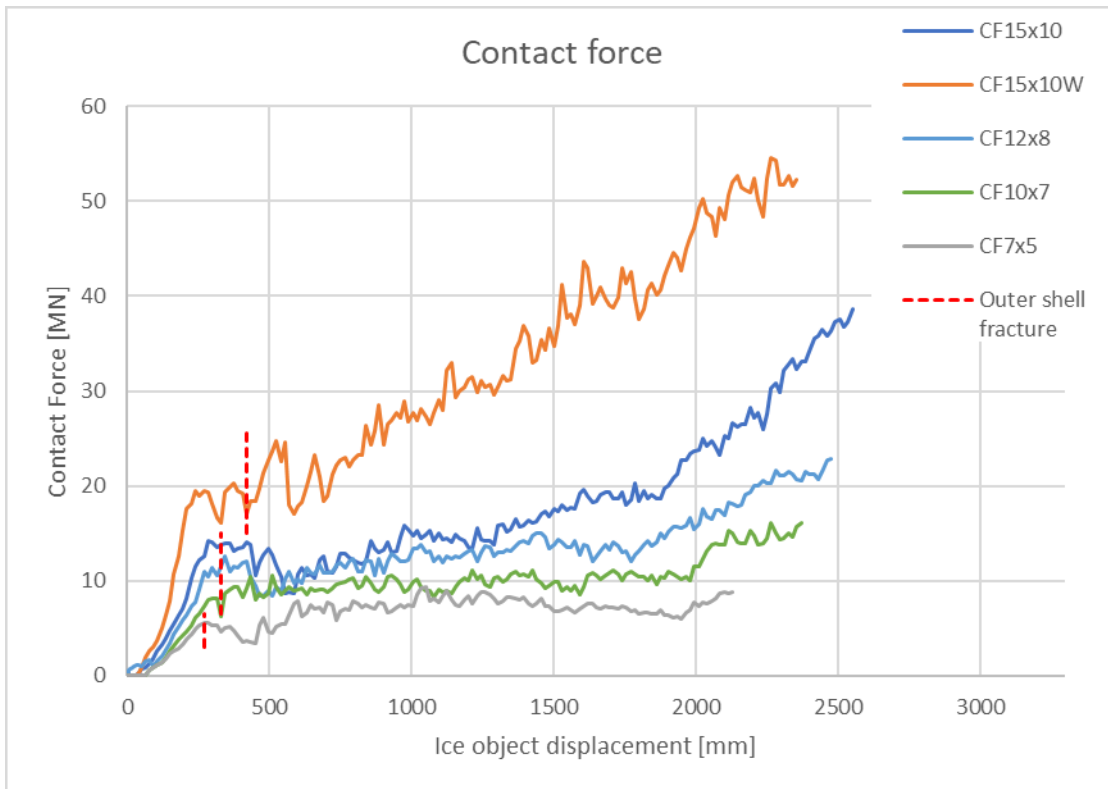

Figure 38: Contact force. The vertical red-dotted lines indicate when the outer shell fractured in each analysis.
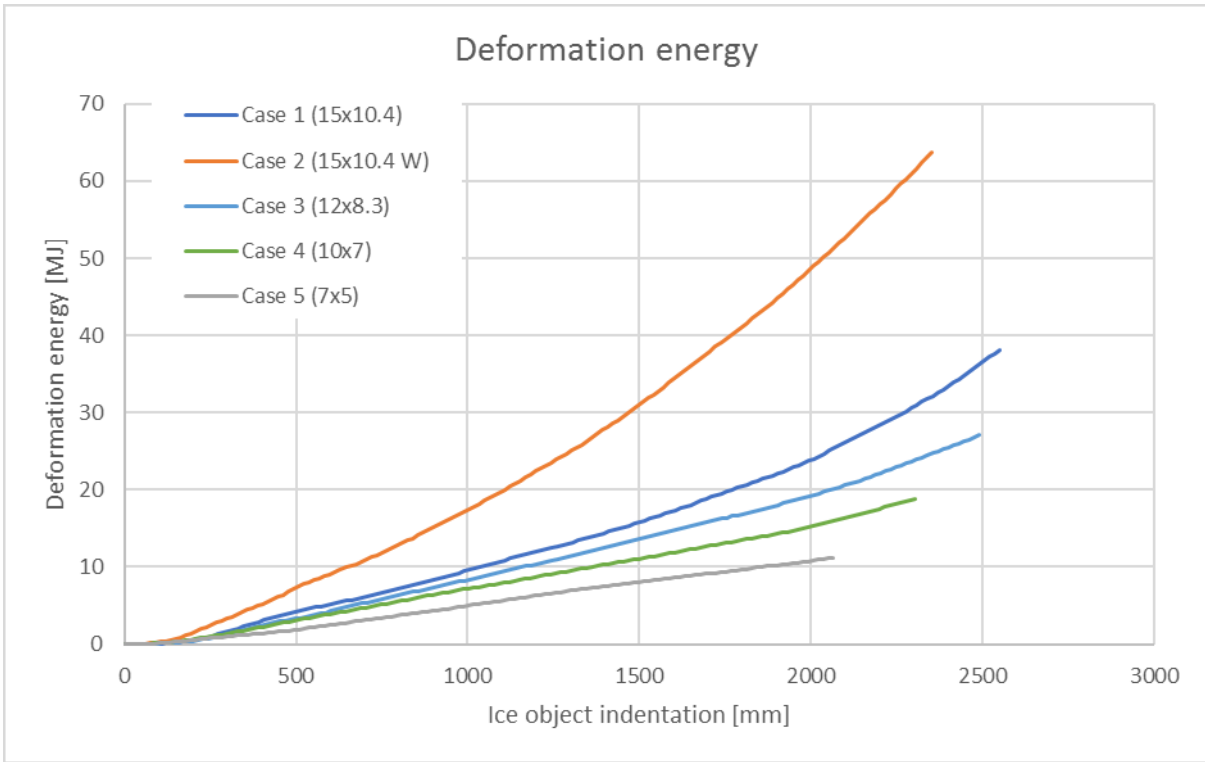
Figure 39: Deformation energy.
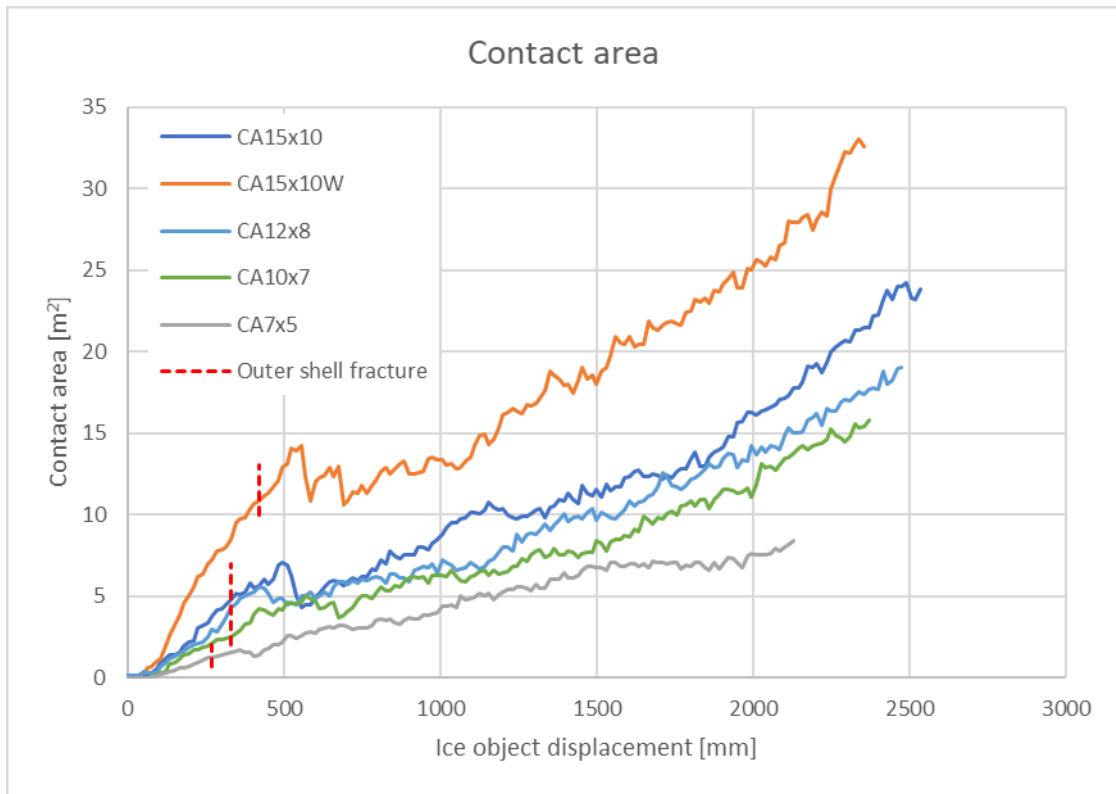
Figure 40: Contact area. The vertical red-dotted lines indicate when the outer shell fractured in each analysis.
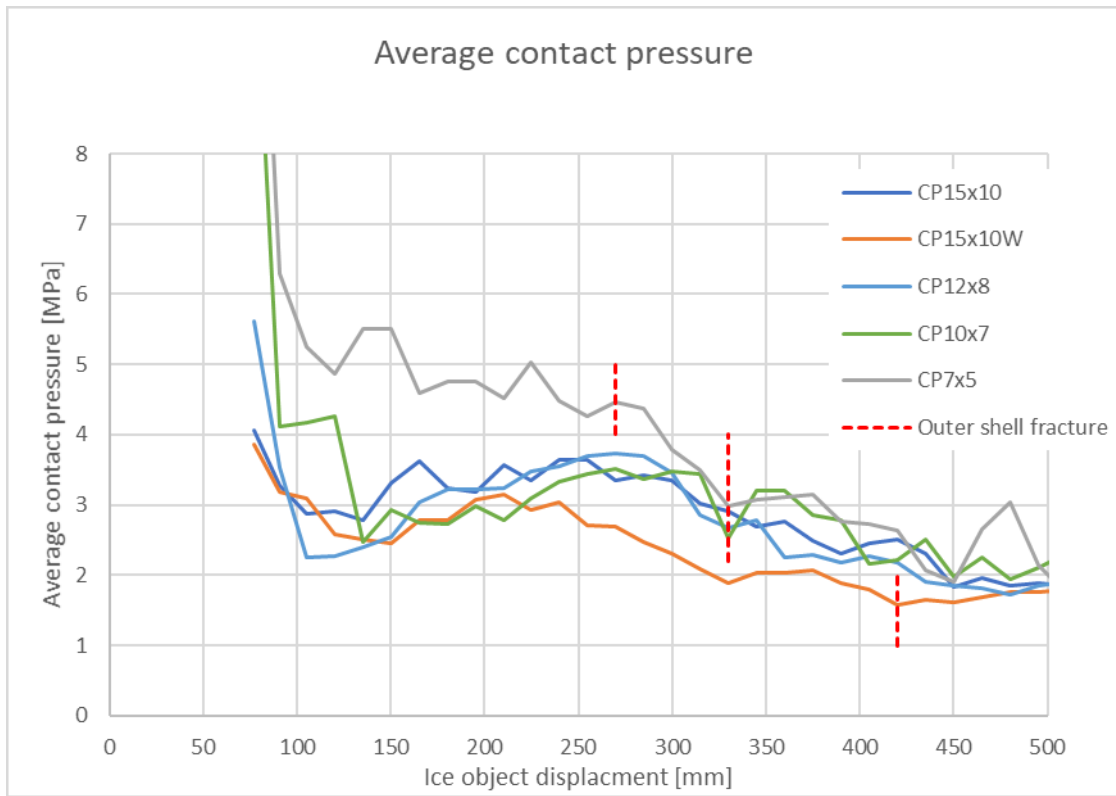
Figure 41: Average contact pressure. The vertical red-dotted lines indicate when the outer shell fractured in each analysis.
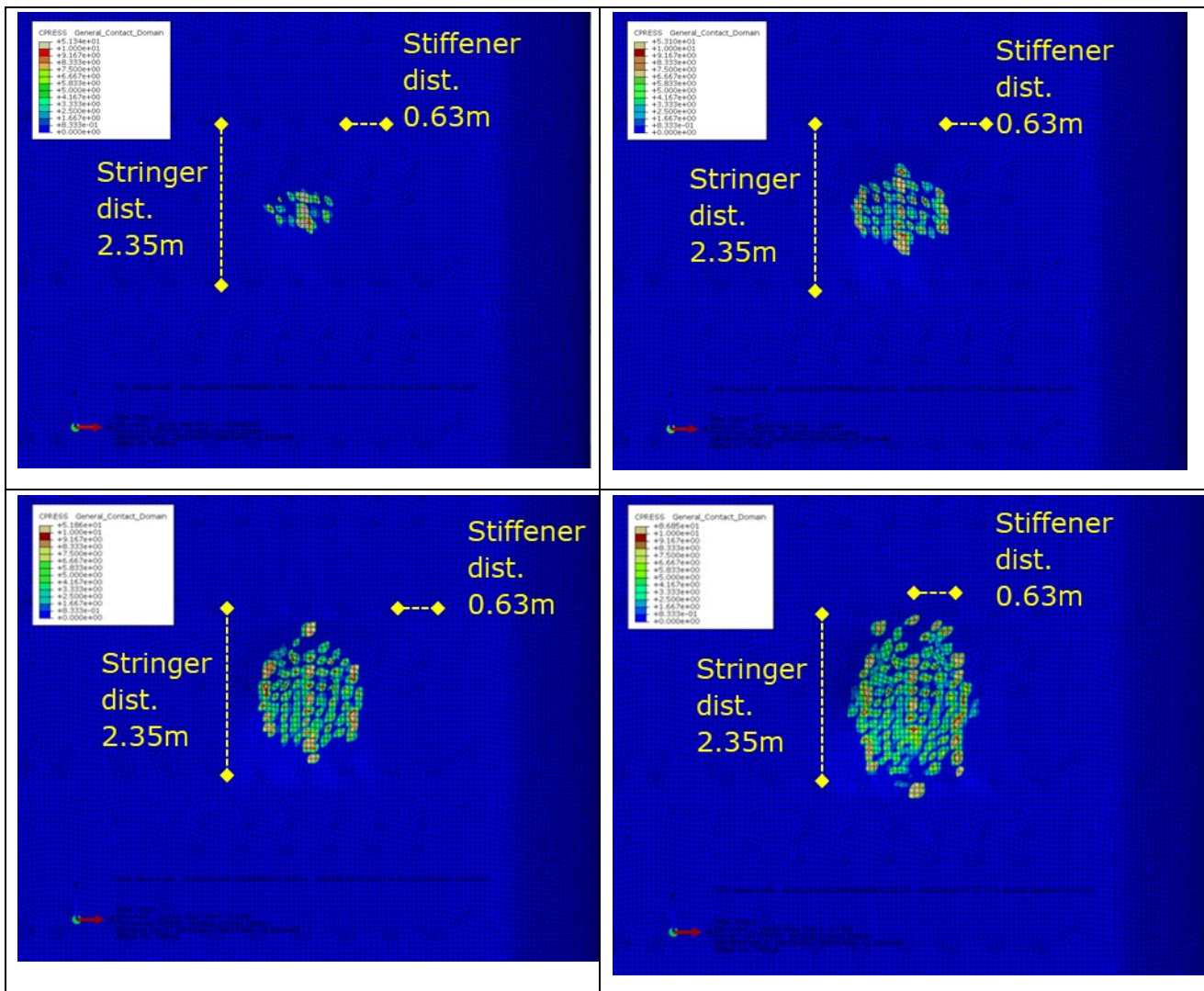
Figure 42: Development in contact area and pressure for case 15x10.4 for deformations: 53 mm, 113 mm, 172 mm and 232 mm (fracture in outer shell).

8.3.4 Analysis, uniform pressure

8.3.4.1   Analysis setup

As an alternative to the rigid object analyses, one analysis with uniform pressure was also performed. The pressure distribution was defined as shown in Figure 43, corresponding to a contact area of 4.45 m², which is roughly the same area as shown for the last step in Figure 42 (at outer shell fracture). The purpose of this analysis was to investigate if a uniform pressure gives a significant different response than a forced deformation following the shape of the rigid object. The pressure was increased until fracture of the outer shell.
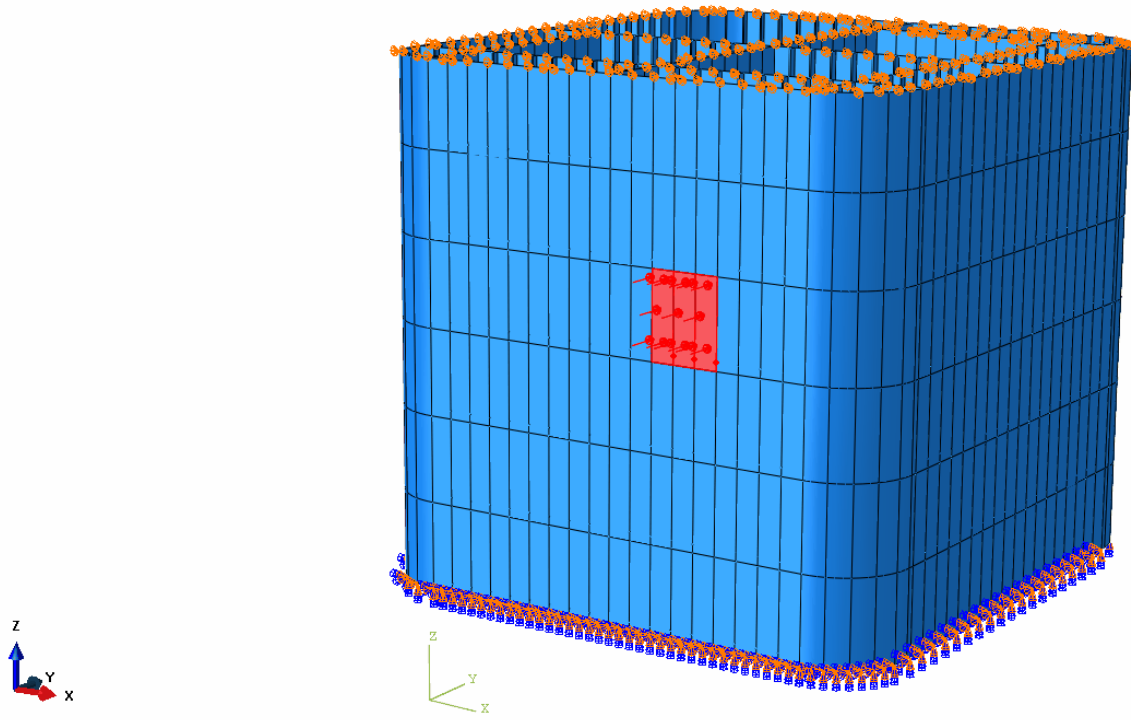
Figure 43: Analysis setup, uniform pressure.

8.3.4.2 Result

The outer shell fractured at a pressure of 3.2 MPa in this analysis. This is in the same order as the average pressure at outers shell fracture for the rigid object analyses. The maximum deformation was 220 mm when the outer shell fractured (Figure 44).
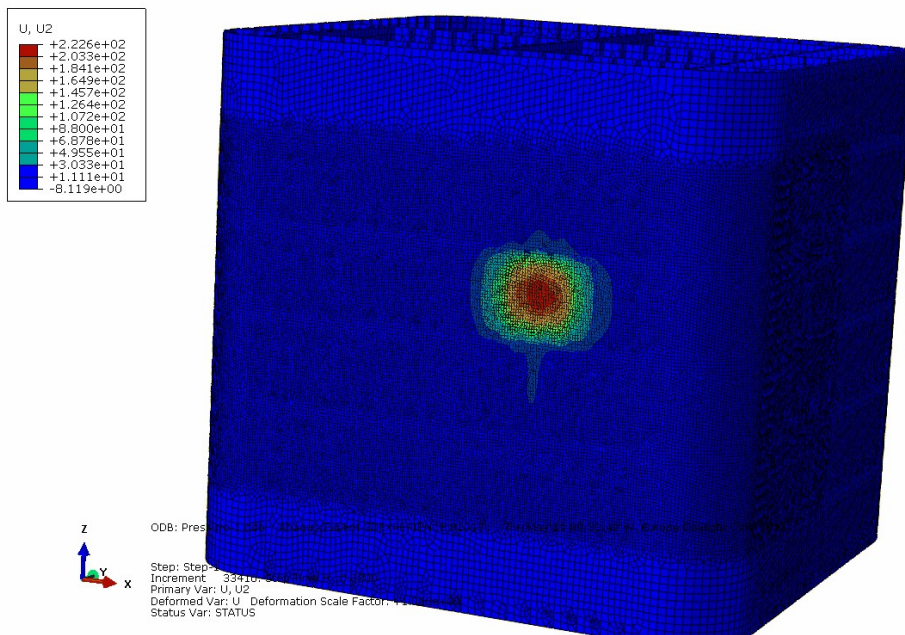
**Figure 44: Maximum deformation before fracture.**

8.3.5 Summary

A section of a column in typical drilling rig suitable for harsh weather operations was modelled.

Five collision analyses with rigid spherical Ice objects and one analysis with uniform pressure was performed. As expected the contact force and the deformation energy increase with increasing size of the impacting object. The estimated maximum deformation before fracture of outer shell was not sensitive to the object size. The outer shell fractured at approximately 300 mm indentation in all cases. A slightly larger deformation before fracture was seen for the "broadside" case (15x10W), for this case a larger area of the outer shell is deformed. The analyses show that approximately 3 MPa is the average pressure the column structure can withstand before the outer shell fractures. The failure mode is membrane tensile fracture, and the result is thus sensitive to the selected fracture limit.

From the pressure plots it is observed that the pressure distribution is far from uniform. The hard points in the structure attracts more loads that the softer parts. To investigate the effect of this an additional analysis where a uniform pressure was applied and gradually increased until outer shell fracture. The resulting maximum pressure was 3.2 MPa, which is similar to the average pressures found for the rigid object analyses.

For comparison with pressure-area model results (Section 7), the pressures were also calculated based on the projected area of the glacial Ice object at "undeformed" outer surface of the facility. The resulting areas becomes larger than what Abaqus calculates from the contact surfaces, Figure 45.
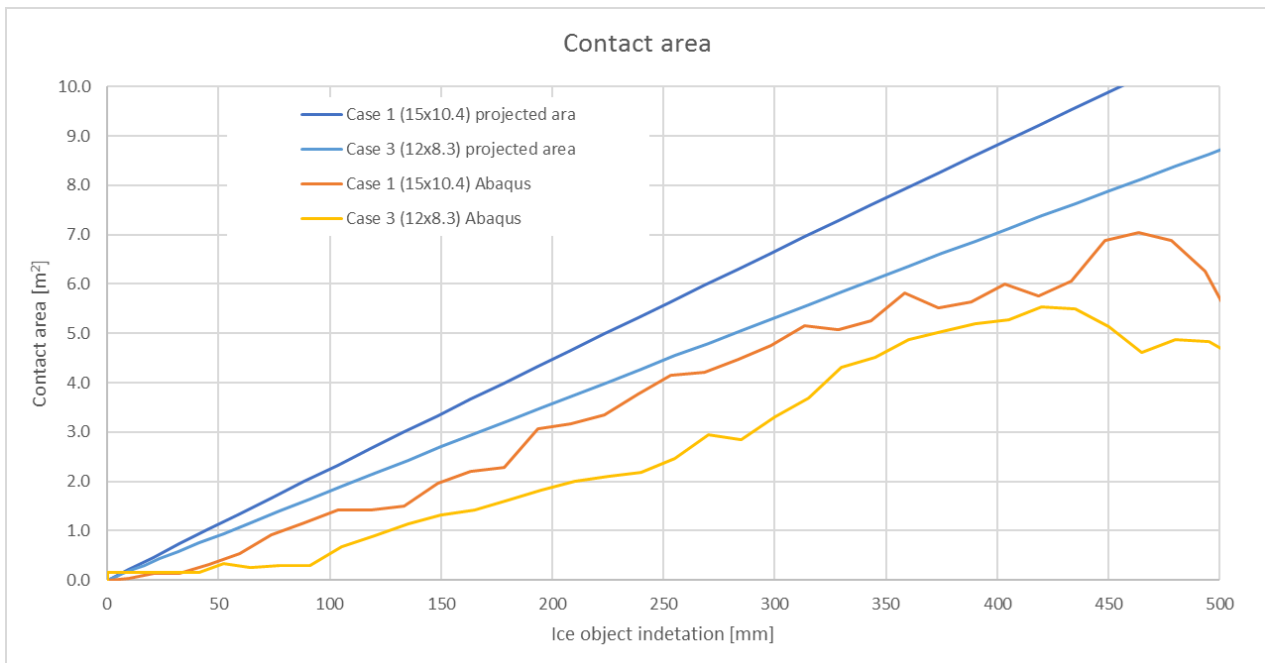
Figure 45: Contact area comparison, calculated by Abaqus vs. projected ice area.

8.4 Evaluation of strain energy dissipation

To assess the dissipation of the strain energy the average "capacity" pressure from FE analyses is compared to the crushing pressure from the pressure-area model (power law with $C_p = 7.4$ and $D_p = -0.7$). As the area to be used in the pressure-area model is a projected area, two plots are prepared:

- In Figure 46 the FE contact pressure is calculated based on the impact forces from FE and nominal contact area from the pressure-area model (projected area).

- In Figure 47 the Ice crushing pressure is calculated based on contact area reported from the FE analyses.

As seen from both figures, the ice crushing pressure is initially larger than the average pressure from the FE analyses. Local deformations in the column must thus be expected. As the contact area increases, the ice crushing pressure (Ch. 7) decrease more than the average "capacity" pressure from the FE analyses and it is likely that energy dissipation will take place in the Ice object (such as crushing). However, as discussed in Chapter 7, the ice crushing pressure to be used is uncertain. More conservative C_p and D_p parameters will quickly result in a clear *ductile design* situation for the facility, where all the energy must be absorbed as deformation energy in the facility.

Comparing the kinetic impact energies found in Chapter 5 with the analysis results in Section 8.3.3, assuming all kinetic energy have to be absorbed as deformation energy in the facility results in the indentation depths given in Table 15. The indicated indentation depths are likely conservative, as hard points in the facility column will partly crush the ice.

From Table 15 it is seen that the shape of the object and thereby the contact area influence how far into the platform column the Ice object penetrates for a given kinetic energy (Case 1 vs Case 2). Pointed rigid ice objects may therefore penetrate further into the facility than larger rigid ship bows, for the same kinetic energy.

Table 15: Indentation depth to absorb all kinetic energy.

	Ice object	Kinetic energy [MJ]	Indentation depth [m]
Case 1	Spheroid 15x10.4	16	1.5
Case 2	Spheroid 15x10.4W	16	1.0
Case 3	Spheroid 12x8.3	9	1.0
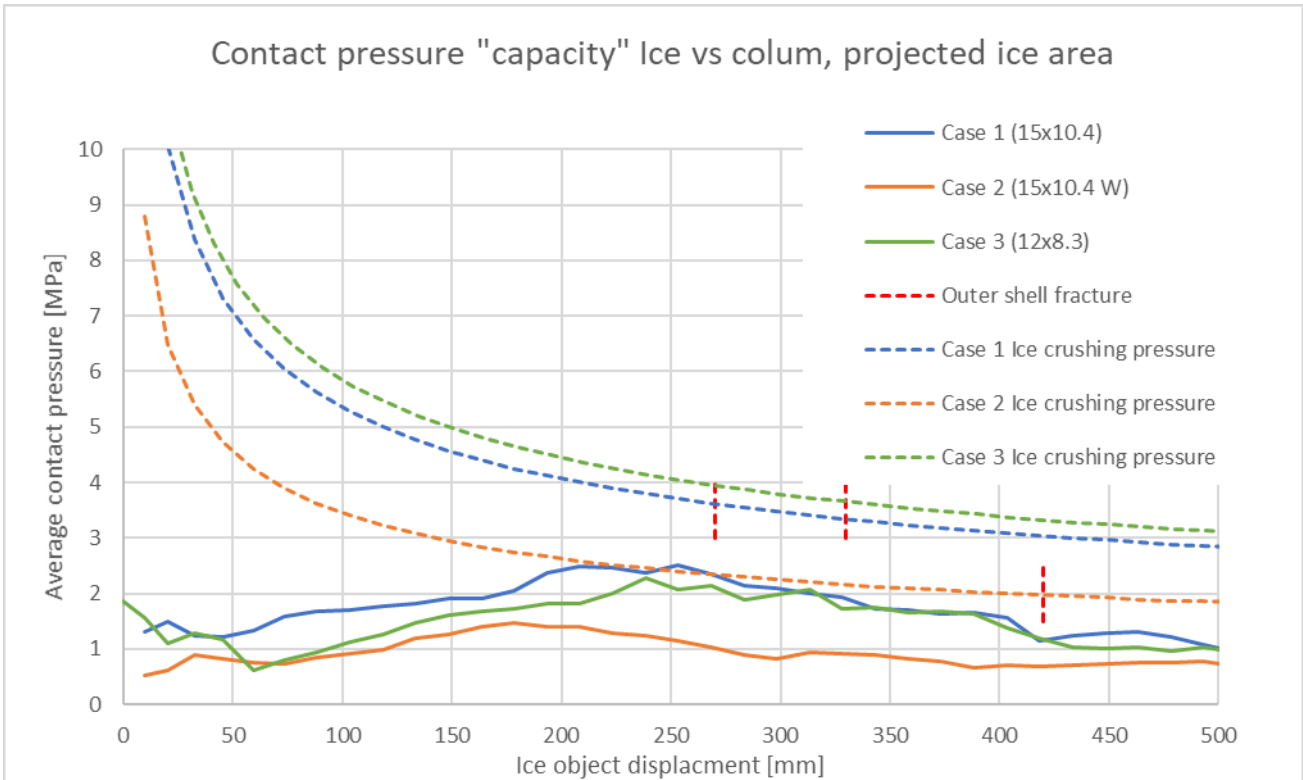
Figure 46: Contact pressure curves with respect to the penetration depth of glacial ice impact with semi-submersible. Curves based on nominal projected ice area.
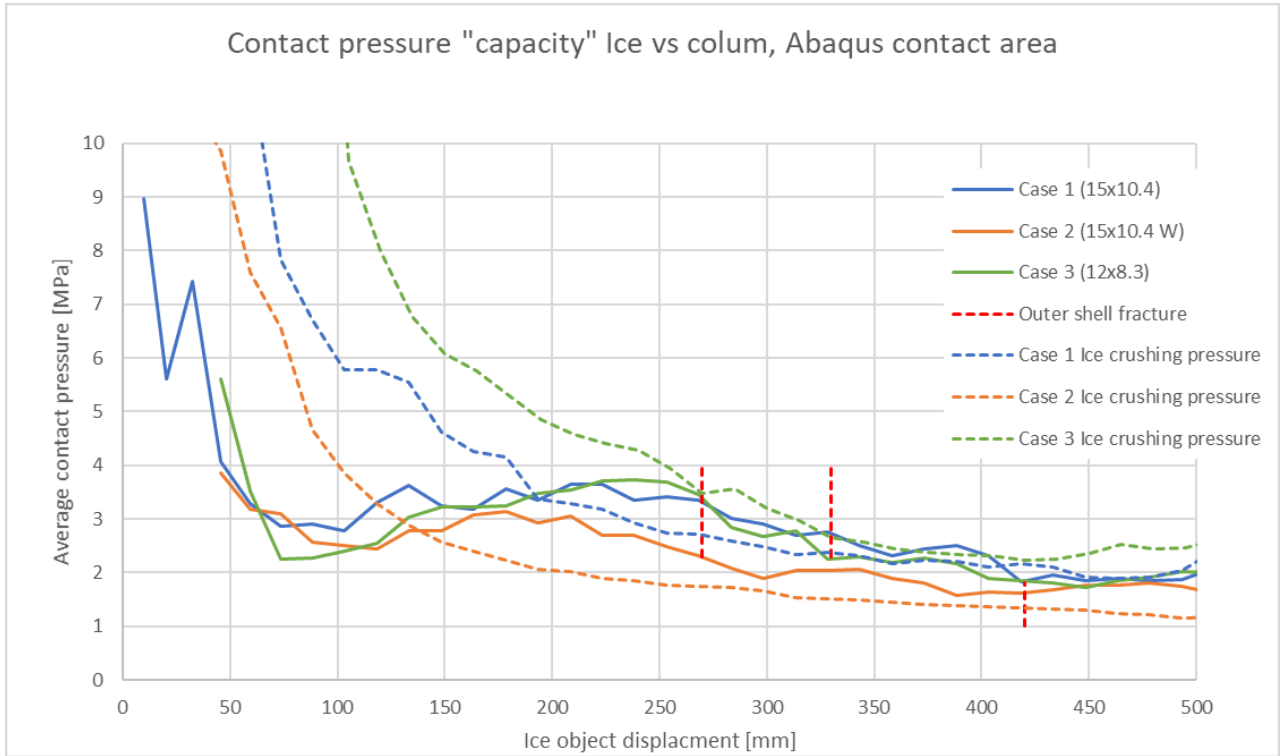
Figure 47: Contact pressure curves with respect to the penetration depth of glacial ice impact with semi-submersible. Curves based on Abaqus contact area.

8.5 Recommendations

Until Glacial ice load models suitable for integrated analyses are available, the main options to evaluate a facility's ability to resist ice collision is to simulate the Glacial ice as

- Rigid objects, as shown in section 8.3.3

- Pressure as function of time as shown in section 8.3.4

The resistance results must then be compared with predicted ice pressure, e.g. pressure-area model results as shown in 7.

Both methods are simplifications and assumes that the structure response and the ice response to the collision can be threated independently. When a "strength design" is aimed for, simulation the ice load using pressure as function of time is a good approximation.

Integrated analyses, where FE models, smoothed-particle hydrodynamics (SPH) or similar are utilized to describe also the crushing of the ice has been attempted by researchers [29] [27] [28]. Data needed to calibrate such advanced models are however scarce, and the models are thus not evaluated to be suited for design against ice collision so far.

9 STABILITY REQUIREMENTS

9.1 General

The NMA stability requirements are specified in "Stability, watertight subdivision and watertight/ weathertight closing means on mobile offshore units (12/20/1991 0878)". The stability requirements in the IMO MODU Code [15], which are included in DNVGL-OS-C301, divides into two sections:

- *Section 3.4: subdivision and damage stability*

- *Section 3.5: extent of damage*.

The requirements in IMO MODU and NMA are not directly comparable and compliance must be shown for both sets of regulations if this is the target.

For assessment of the stability when interacting with glacial ice the existing requirements to damage stability, as described by NMA, may be sufficient for assessment of interaction with glacial ice. This is not considered in detail here. However, an important input to the damage analysis is the extent of damage.

9.2 Extent of damage

The extent of damage considered for a ship impact is not sufficient when considering an impact with glacial ice. Glacial ice may impact both above and below the zone which are required to withstand a ship impact. Smaller glacial ice pieces may also enter in-between the legs of a semi-submersible and impact on elements assumed sheltered against a ship impact. Examples here are the backside of the columns and the drill string. The present study shows that the extent of damage need to be revised in order to account for impact between an installation and glacial ice pieces. Table 16 summarize whether the extent of damage considered in the current NMA regulations for stability analysis are sufficient for glacial ice impact investigations.

Table 16: Assessment of the application of damage requirements for ship impact for glacial ice impact stability investigations.

	Extent of damage to consider after NMA	Glacial ice
1	Only those columns and pontoons on the periphery of the unit shall be assumed open to damage, and it is assumed that damage will only occur to «exposed parts». «Exposed parts» are those portions of columns and pontoons, or other parts providing buoyancy which are located outside a line drawn through the centres of the peripheral columns (see Figure 2).	May not be sufficient for glacial ice impact. Not considered in detail. See Section 5.2.
2	Vertical extent: 3.0 m within 5 metres above and 3 metres below the waterline in question.	Extent not sufficient for glacial ice. See Section 6.2. Damage in more than 2 compartments not assessed.
3	Horizontal extent: 3.0 m measured along the periphery of the shell.	Not considered
4	Penetration: 1.5 m measured at a right angle to the shell.	May not be sufficient. See section 8.4.

9.3 Requirements for glacial ice impact assessments

This study assessed selected shapes and sizes of glacial ice combined with three 100-year return period sea-states (Figure 6). The return period for the joint event that glacial ice impacts a facility in a 100-year sea state is probably greater than 100 years. However, the horizontal penetration and the vertical extent of an impact from glacial ice on a facility may still be greater than that estimated in this study and depends on several factors whereof the geographical location is the most important.

The study shows that the existing requirements for ship impact assessment are not sufficient to account for an impact between glacial ice and a semi-submersible. The analysis in this study is not sufficient to propose new requirements but clearly identify that the requirement to extent of damage would need to be revised to account for impacts with glacial ice. The example in this study shows that the impact can occur both above and below the vertical extent required for ship impact assessments. In addition, smaller pieces of glacial ice may drift in-between the legs of a semi-submersible and impact on area normally considered sheltered against an impact.

The horizontal penetration depth may also be greater than 1.5 m (section 8.4). The latter depends on the applicability of the model that is used to describe the interaction between glacial ice and the facility. There is considerable uncertainty associated with the use models describing the interaction between the glacial ice and the facility. This uncertainty transfers to in-conclusive results regarding which body that is being deformed, the glacial ice or the facility or both.

10 CONCLUSION

The main objective with this study was to clarify the relevance of the inherent capacity of a facility to withstand a ship impact when considering impact with glacial ice. As an example, interaction between a semi-submersible and glacial ice was investigated.

Glacial ice with a waterline length of maximum 15 m and with either an elliptical or cuboid shape was used in the assessment. The limited size of glacial ice, which correspond to bergy bits and growlers, was chosen to reflect the reduced possibility for an iceberg management system to detect and avoid an interaction with small glacial ice pieces in waves.

The main findings in this study are the following:

- vertical extent of damage assumed for ship impact assessment is not sufficient for glacial ice impact assessments

- structural components assumed not to be exposed to ship impact may be exposed to impact from glacial ice

- the horizontal penetration of damage may exceed 1.5 m which is the minimum requirement for ship impact

- the pressure-area formulation used to assess glacial ice impact is associated with uncertainty that should be considered in estimating glacial ice loads

Wadam analysis shows that the vertical extent assumed for ship impact is not sufficient to cover the possible extent of damage resulting from interaction between glacial ice and a semi-submersible. This is supported by analysis with a 100 year-sea state for all shapes and sizes and the same was observed using 1 and 10-year sea states for a cuboid. Further work is required to propose limits for the vertical extent of damage to be considered but the results show that the impact may occur both above and below the limits used for ship impact assessments. Non-linear hydrodynamic effects, like varying water plane area through the wave cycle, are studied for the large spheroid with the program Wasim. The results show that the vertical motion and horizontal velocity is increased compared with the Wadam analysis. Also, it is observed that the spheroid may be completely submerged and the pitch time series show full turns. However, the validity of the Wasim results are questionable when the spheroid is completely submerged and rotating full turns.

The assumption that impact only occurs on the outer perimeter of the facility is questionable for impacts with glacial ice. Glacial ice comes in many sizes and shapes and may protrude in-between the legs of a semi-submersible. In such a case, it may interact with structural elements not required to withstand ship impacts. The possibility for damage on more than two compartments has not been assessed in this study but the variability of the shapes and sizes of glacial ice suggests that a damage in more than two compartments cannot be excluded.

For ship impact the horizontal penetration of damage shall be assumed to be 1.5 m, this may not be sufficient for glacial ice impact. A finite element analysis which assumes that all dissipation of energy goes into the facility, shows that relatively low impact energies may cause significant penetration. The estimated horizontal penetration depth depends on the geometry of the glacial ice, the energy available for deformation and the pressure exerted by the ice on the facility. There is considerable uncertainty associated with the pressure-area relation for glacial ice and further work is required to conclude on this matter.

The main options to evaluate a facility's ability to resist ice collision is to simulate the Glacial ice as

- Rigid objects

- Pressure as function of time

The resistance results must then be compared with predicted ice pressure, e.g. pressure-area model results as shown here.

Both methods are simplifications and assumes that the structure response and the ice response to the collision can be threated independently. When a "strength design" is aimed for, simulation the ice load using pressure as function of time is a good approximation. There is considerable uncertainty associated with the pressure-area relation for glacial ice and further work is required to conclude on this matter.

Integrated analyses (non-linear), where FE models, smoothed-particle hydrodynamics (SPH) or similar are utilized to describe also the crushing of the ice has been attempted. Data needed to calibrate such advanced models are however scarce, and the models are thus not evaluated to be suited for design against ice collision so far.

11 REFERENCES

[1] DNV GL, "Aspect of structural safety in the Barents Sea, Report No. 2016-0648, Rev. 2," DNV GL, 2016.

[2] DNV GL, "Towards a Framework for Ice Load Factor Calibration, Relevant to Structural Design of Floating Arctic Offshore Installations on the Norwegian Continental Shelf (NCS), Report No. 2017-1173, Rev. 0," DNV GL, 2017.

[3] Canadian Ice Service, "Manual of Standards Procedures for Observing and Reporting Ice Conditions," Canadian Ice Service, 2015.

[4] Det Norske Meteorologiske Institutt, "avisnomenklatur (Den Meteorologiske Verdensorganisasjons beskrivelse av istyper på havet) (WMO Sea Ice Nomenclature Norwegian Edition)," Det Norske meteorologiske Institutt, 1982.

[5] Petroleum Safety Authority, *The Framework Regulations,* Petroleum Safety Authority, 2016.

[6] Petroleum Safety Auhority, *Facility Regulations,* Petroleum Safety Auhority, 2015.

[7] Norwegian Maritime Authority, "Regulations: https://www.sjofartsdir.no/en/shipping/legislation/#regulations".

[8] DNV GL, "Offshore drilling and support units, DNVGL-RU-OU-0101," DNV GL, 2017.

[9] DNV GL, "Structural design of offshore units - WSD method, DNVGL-OS-C201," DNV GL, 2016.

[10] DNV GL, "Structural design of column stabilized units - LRFD method, DNVGL-OS-C103," DNV GL, 2015.

[11] DNV GL, "Verification for compliance with Norwegian shelf regulations, DNVGL-SI-0166," DNV GL, 2016.

[12] Standards Norway, "NORSOK N-003, Action and action effects," 2017.

[13] Standards Norway, "NORSOK N-003, Action and action effects," Standards Norway, 2007.

[14] Norwegian Maritime Authority, "Regulations of 20 December 1991 No. 878 on stability, watertight subdivision and watertight/weathertight means of closure on mobile offshore units," 2016.

[15] IMO MODU CODE, "Code for the contruction and equipment of mibile offshore drilling units," International Maritime Organization, 2009.

[16] DNV GL, "Stability and watertight integrity, DNVGL-OS-C301," DNV GL, 2017.

[17] DNV GL, "Design of offshore steel structures, general - LRFD method, DNVGL-OS-C101," DNV GL, 2016.

[18] Rossiter et al., "Remote sensing ice detection capabilities - East Coast," Environmental Studies Research Funds, Calgary, 1995.

[19] Barents Sea exploration collaboration, "Fysisk miljø i Barentshavet sørøst," https://www.norskoljeoggass.no/no/Faktasider/Miljo1/Barents-Sea-Exploration-Collaboration/Metocean-and-Ice/, 2016.

[20] DNV GL, "Environmental Conditions and Environmental Loads, DNVGL-RP-C205," DNV GL, 2017.

[21] R.-Q. Lin and W. Kuang, "A fully nonlinear, dynamically consistent numerical model for solid-body ship motion. I. Ship motion with fixed heading," *Proc. R. Soc. A,* 2010.

[22] D. E. Newland, Random Vibrations, Spectral and Wavelet Analysis, Dover Publications, Inc., 2005.

[23] DNV GL, "WASIM Wave Loads on Vessels with Forward Speed," DNV GL AS, 2017.

[24] DNV GL, "Design against accidental loads, DNVGL-RP-C204," DNV GL, 2017.

[25] Veritec, "Design guideline for offshore steel structures exposed to accidental loads, Rep. No. 88-3172," Vertiec (Det Norske Veritas), 1988.

[26] DNV GL, "Determination of structural capacity by non-linear finite element analysis methods, DNVGL-RP-C208," DNV GL, 2016.

[27] Z. Liu, "Analytical and Numerical Analysis of Icebergs Collisions with Ship Structures," Norwegian University of Science and Technology, Trondheim, Norway, 2011.

[28] E. Kim, "Experimental and Numerical Studies Related to the Coupled Behaviour of Ice Mass and Steel Structures during Accidental Collisions," Norwegian University of Science and Technology, Trondheim, Norway, 2014.

[29] N. Ferrari, E. Rizzuto and A. Prestileo, "Modelling ice characteristics in iceberg-ship collision analyses," in *16th International Congress of the International Maritime Association of the*

Mediterranean, Pula, Croatia, 2015.

[30] SIMULIA, "Dassault systems: Abaqus 2017," [Online]. Available: https://www.3ds.com/products-services/simulia/products/abaqus/.

[31] ISO 19906, "Petroleum and natural gas industries - Arctic offshore structures," International Organization of Standardization, Geneva, Switzerland, 2010.

About DNV GL

Driven by our purpose of safeguarding life, property and the environment, DNV GL enables organizations to advance the safety and sustainability of their business. We provide classification and technical assurance along with software and independent expert advisory services to the maritime, oil & gas and energy industries. We also provide certification services to customers across a wide range of industries. Operating in more than 100 countries, our professionals are dedicated to helping our customers make the world safer, smarter and greener.